

MATERIAL AND MECHANICAL ENGINEERING TECHNOLOGY

Editorial board of the journal

Gulnara Zhetessova (Karaganda State technical University, Kazakhstan) (chairman)

Alexander Korsunsky (University of Oxford, England)

Olegas Cernasejus (Vilnius Gediminas Technical University, Lithuania)

Jaroslav Jerz (Institute of Materials & Machine Mechanics SAS, Slovakia)

Boris Moyzes (Tomsk Polytechnic University, Russia)

Nikolai Belov (National Research Technological University "Moscow Institute of Steel and Alloys", Russia)

Georgi Popov (Technical University of Sofia, Bulgaria)

Sergiy Antonyuk (University of Kaiserslautern, Germany)

Zharkynay Christian (University of Texas at Dallas Institute of Nanotechnology, USA)

Katica Simunovic (University of Slavonski Brod , Croatia)

Lesley D.Frame (School of Engeneering University of Connecticute, USA)

Olga Zharkevich (Karaganda State Technical University, Kazakhstan) (technical secretary)

Content

Kyzyrov K.B., Reshetnikova O.S., Dosmagambetov N.G. Modeling and Calculating the Fluid Distribution System Parameters of Hydraulic Hammer VKP.250.....	3
Komissarov A.P., Nabiullin R.Sh. Analyzing Common Transmission Mechanism of the Mining Excavator Main Mechanisms Drives	8
Pak Yu.N., Pak D.Yu., Tebayeva A.Yu., Malikov N.M. Studying Gamma-albedo Method Sensitivity to Control Effective Atomic Number of Complex Materials.....	12
Gavrilin A.N. Development of a Mathematical Model of a Device for Cleaning Road Surfaces from Ice.....	16
Bukanov Zh.U. Research of the Process of Obtaining Blanks by Combining Casting and Heading.....	23
Ashkeyev Zh.A. Research of the Mechanism of Hardening of Liquid Metal in a Crystallizer During Casting and Extrusion Machine.....	29

Modeling and Calculating the Fluid Distribution System Parameters of Hydraulic Hammer VKP.250

Kyzyrov K.B., Reshetnikova O.S.* , Dosmagambetov N.G.

Karaganda Technical University, Kazakhstan

*corresponding author

Abstract. The article is dealing with studying the parameters of the fluid distribution system of the hydraulic hammer VKP.250, the design of which was developed within the framework of the grant project. The research was carried out on a simulation model of a hydraulic hammer built in the PC SolidWorks. Simulation modeling made it possible to determine the design parameters of the fluid distribution system, such as the diameters of the control channels for switching the spool, the width of the control grooves in the hammer body, to analyze changes in pressure, speed and temperature in the front and rear chambers of the hydraulic hammer, control channels and fluid distribution.

Keywords: hydraulic hammer, striker, spool, modeling, simulation model.

1. Introduction

At present, thanks to new technologies and the development of computerization, design, calculation, performance testing, the analysis of the output parameters of new technological equipment including hydraulic impact devices can be carried out by means of building a simulation model in the corresponding applied complex [1].

The use of new computer technologies makes it possible to reduce the time required for preparing the tests; to reduce material consumption and, accordingly, financial costs, especially when designing large-sized objects; to perform experiments in critical modes, which would lead to the destruction of the physical layout, etc.

The analysis of works dealing with studying hydraulic percussion devices shows that when studying the characteristics of the working cycle of strikers, the authors resorted to the development of a mathematical model of the striker and spool movement. The mathematical model is in the general case the second-order differential equation, for the solution of which the authors make appropriate assumptions, which can lead to errors in solving differential equations [2-5].

Simulation modeling allows recreating an exact copy of the object under study, taking into account all the factors affecting its characteristics. The present work is dealing with this very task, the purpose of which is to study and to analyze the parameters of an experimental model of the VKP.250 hydraulic hammer.

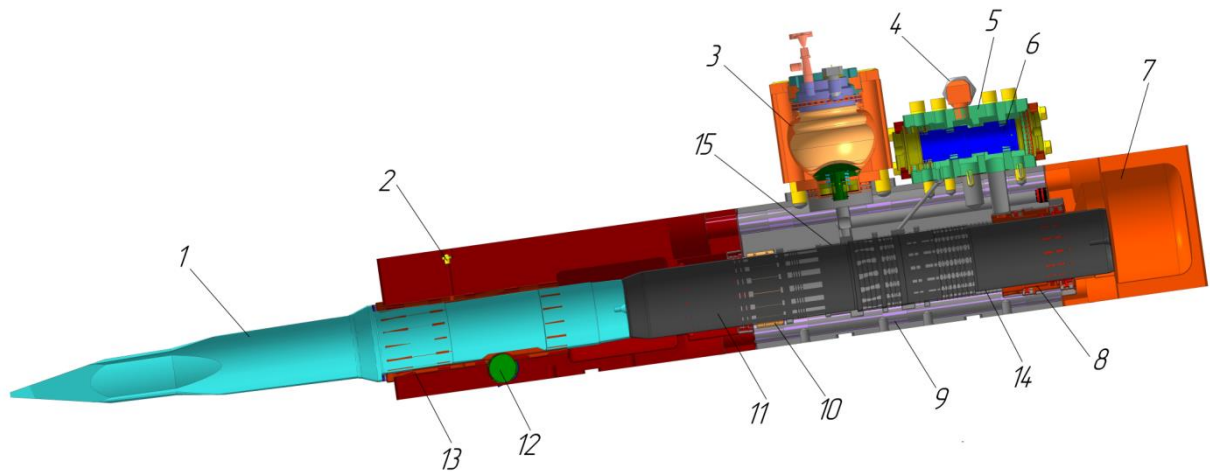
2. The study aim

The design of a prototype hydraulic hammer VKP.250 was developed within the framework of the grant theme "Developing and studying a hydraulic impact mechanism for mining and construction work" by the Ministry of Education and Science of the Republic of Kazakhstan order for 2018-2020. The general view of the VKP.250 hydraulic hammer is shown in Figure 1.

In order to ensure manufacturability and maintainability, the hydraulic hammer is divided into several blocks: tool block 1; hydraulic block 9 with a communications system; gas chamber 7; mains battery 3; control block 5; regulation block [6, 7].

The hydraulic hammer has two chambers: front (idle) chamber 15 that is always under pressure of the working fluid, and rear (working) chamber 14 that is alternately connected to the pressure and drain lines. Driven link 11 performs the combined functions of the piston, striker and distributor of the first stage (piston-striker-spool PSS). Three-way distributor of the second stage 5 controlled through the right cavity from the distributor of the first stage, controls the working stroke chamber. The switching of both spools occurs when the driven link reaches a certain position.

The hammer design is compact; it is characterized by the presence of a progressive system of sealing the working chambers by discharging the movable seals; the location of the bearing surfaces of the striker piston on the front and rear rods; the presence of a gas chamber that ensures guaranteed starting of the hammer and smoothing the dynamics of the working fluid in the drain line; manufacturability of the impact-piston group.



1 - tool; 2 - oiler; 3 - mains battery; 4 - fittings for connecting pressure and drain pipelines; 5 - control block body; 6 - spool; 7 - gas chamber; 8, 10, 13 - bronze bushings; 9 - block body with a hydraulic communications system; 11 - striker; 12 - finger; 13 - bushing; 14 - working stroke chamber (rear controlled chamber); 15 - idle chamber (front uncontrolled chamber)

Fig. 1. - Hydraulic hammer VKP.250 in section

3. Analyzing the study results

For the purpose of checking the efficiency of the structure, modeling and calculation of the parameters of the hydraulic breaker fluid distribution system were carried out. To study and to analyze the parameters of the system, the software package "SolidWorks" with an additional module for gas-hydrodynamic calculations "Flow Simulation" was used. A simulation model of the hydraulic hammer is shown in Figure 2. It consists of the following elements: 1 - mains battery; 2 - hydraulic unit; 3 - gas chamber; 4 - control unit; 5 - control unit. The model is built in accordance with the dimensions indicated in the design drawings with specification of the material of the structural elements.

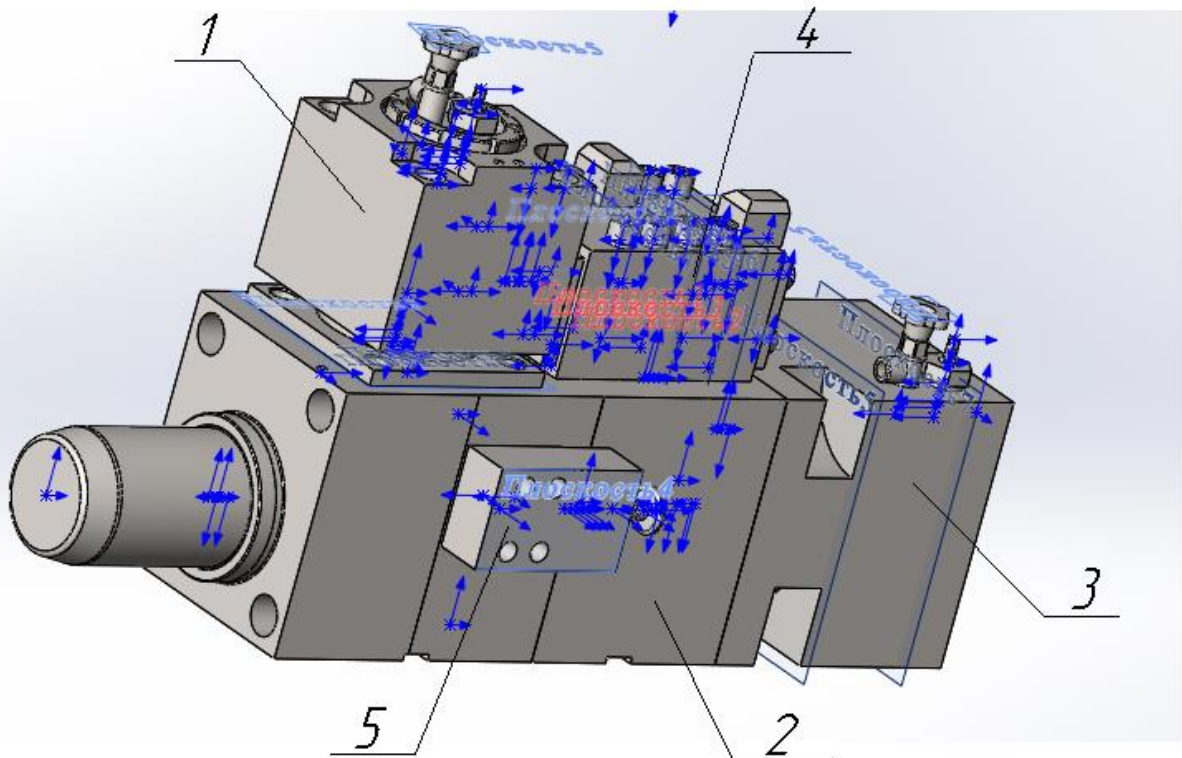


Fig. 2. – Simulation model of the hydraulic hammer

The calculation of the fluid distribution system includes the following main steps:

1. Setting the shape, size and materials of blocks, gas chamber; mains battery;
2. Setting the fixed positions of the striker and spool;
3. Input of initial data;
4. Launching the calculation task;
5. Analyzing the results obtained.

According to the working cycle of the hydraulic hammer, the studies were carried out for four possible positions of the striker and the spool valve of the 2nd stage (Figure 3):

- the 1st position: the striker windup;
- the 2nd position: the 2nd stage spool switching;
- the 3rd position: the beginning of the working stroke - acceleration of the striker;
- the 4th position: the moment of the striker impact with the tool.

The next steps made it possible to select the type of the problem, to set the initial data (Table 1), and to launch the program for calculation.

Table 1 – Initial data

No	Parameters			Parameter description
	Designation	Units	Numerical values	
1	P_g	MPa	2	Gas chamber pressure
2	P_{ch}	MPa	0.6	Battery charging pressure
3	P_w	MPa	16	Working fluid supply pressure
4	P_d	MPa	1	Working fluid drain pressure
5	Q	m^3/s	0.001	Fluid consumption
6	ρ	kg/m^3	865	Working fluid density
7	ν	m^2/s	10^{-5}	Kinematic viscosity coefficient

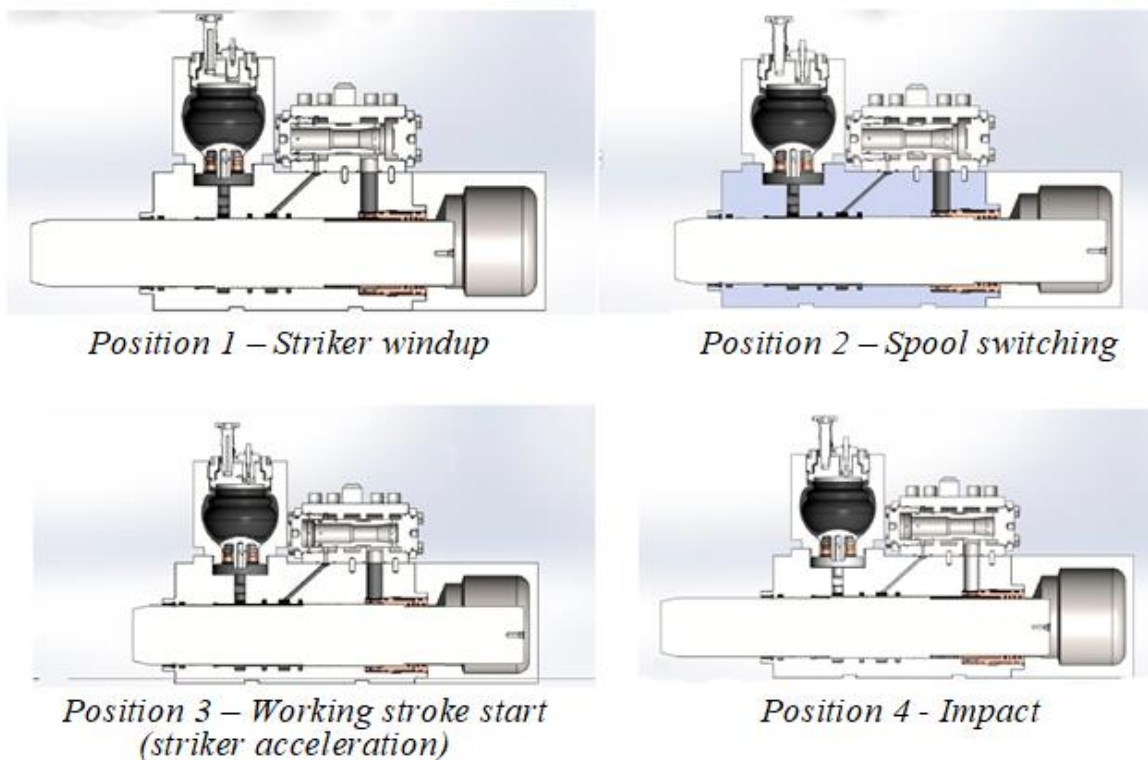


Fig. 3. – Setting the fixed positions of the striker and spool

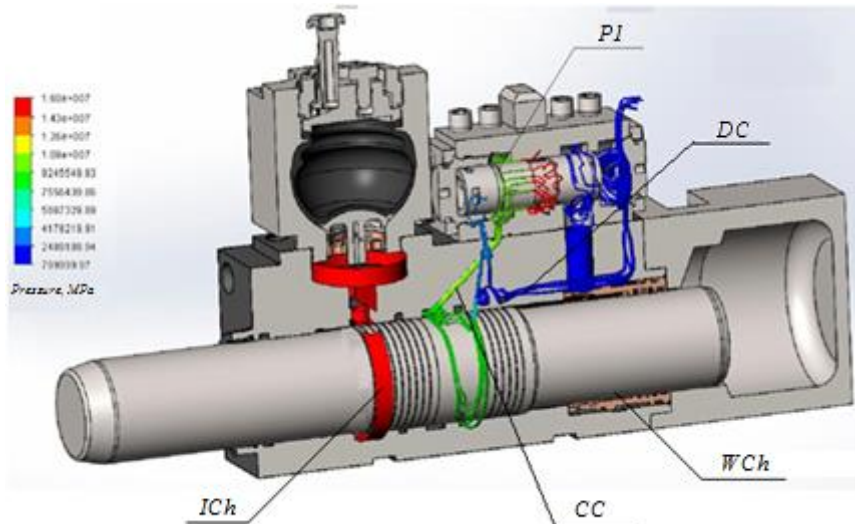
The working fluid is hydraulic oil VMGZ-45 that is widely used in hydraulic pulse technology in production. All the necessary characteristics (density, dynamic viscosity, specific heat, thermal conductivity coefficient) of this oil grade were taken into account.

4. Conclusions

The most visual representation of changing the characteristics of the fluid flow is given by the diagrams, where changing the values of the sought parameters is characterized by coloring in the appropriate color. As a result of calculating the simulation model, an additional design adjustment was made to the hydraulic hammer fluid distribution system.

Let us analyze the results of calculating the parameters of the fluid flow using the example of the obtained data for position 1 (Figure 3). Diagrams of changes in pressure, speed and temperature of the working fluid in the hammer chambers, spool valve control chambers, hydraulic communication system for Position 1 are shown in Figures 4 - 6.

Here, the spool is in the position at which the working stroke chamber is connected to the drain line, and the idle chamber is connected to the pressure one, the striker is in the extreme left position characterizing the windup start.



ICh – idle stroke chamber; WCh – working stroke chamber; CC – control channels; DC – discharge channels; P1 – spool plunger

Fig. 4. – The curve of changing pressure for Position 1

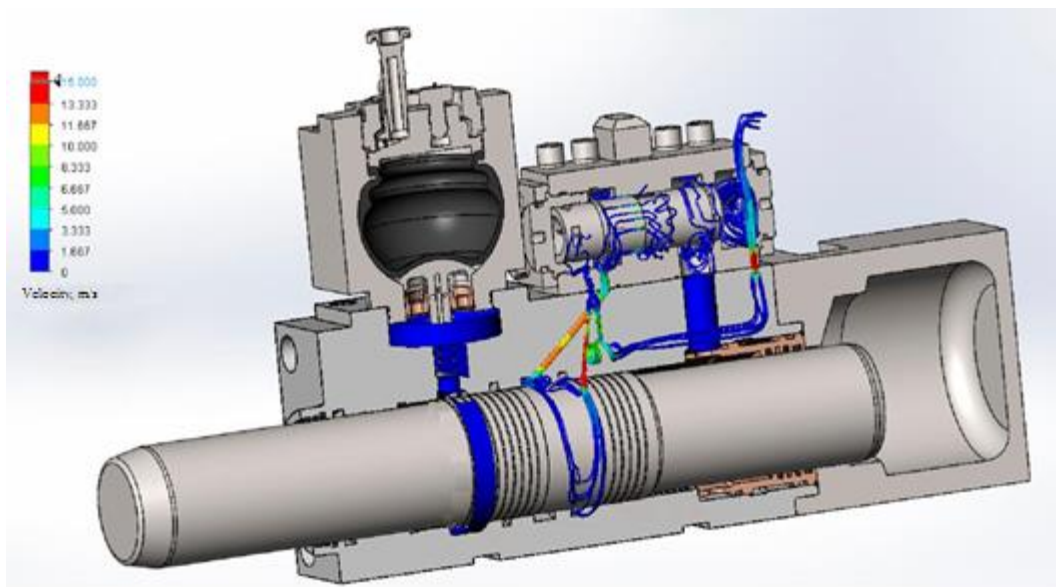


Fig. 5. – The curve of changing the fluid speed in the system of distribution for Position 1

The value of the fluid pressure changes as follows (Figure 4): in the chamber of the working stroke WCh and in the drain line it reaches the value of 1 - 1.5 MPa, in the idling chamber ICh it is 15.5-16 MPa. The mains battery is discharged at this moment. The fluid pressure in the control channels CC connecting the front chamber with the valve cavity for switching the plunger P1 is 9.2 - 10 MPa. Pressure in the discharge channels is 1 - 1.5 MPa.

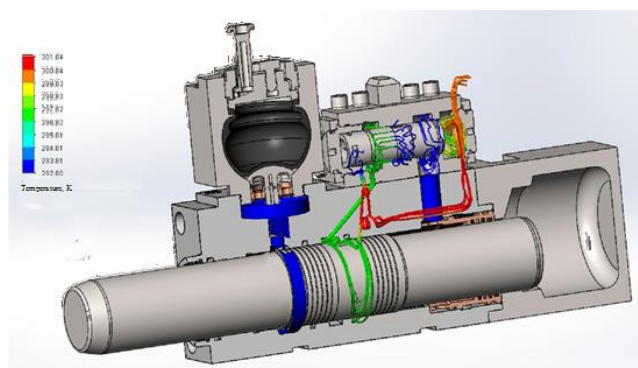


Fig. 6. – The curve of changing the temperature of the fluid in the distribution system for Position 1

The analysis of the results of calculating the speed of the fluid in the channels of the distribution system of the hydraulic hammer (Figure 5) shows that in all the studied positions the average value of the speed is 2 - 3 m/s, in the flow sections of the control channels the value of the speed reaches 10 - 15 m/s.

The temperature change in the hammer chambers and in the hydraulic communication system is insignificant and amounts to 25 - 30 °C. When the fluid is displaced from the distributor channels into the drain pipeline, as well as when the fluid passes through the narrow sections of the channels, its temperature rises due to hydraulic resistance and in some cases can reach 50 °C.

The analysis of the results obtained allows speaking of the adequacy of the obtained characteristics and the operability of the structure.

Studying the parameters of the fluid distribution system of the VKP.250 hydraulic hammer made it possible to establish the design parameters of the hydraulic hammer: the striker stroke h and its mass m , the diameters of striker stages; the diameters and flow cross-sections of the spool valve of the control unit, etc. at the given energy parameters of the fluid flow: power consumption $Q = 60-80$ l/min; engine supply pressure $P_d = 10$ MPa; pressure in the gas chamber 2 MPa; charging pressure of the mains battery $P_a = 0.6$ MPa.

Thus, the main parameters were established, which are the basis for the design implementation of the selected design scheme of the VKP.250 hydraulic hammer.

5. References

- [1] Nesterenko E.S. Basics of computer-aided design systems. Ministry of Education and Science of Russia, CSAU n.a. S.P. Korolev. - Samara, 2013. - 56 p.
- [2] Redelin R.A. Increasing the efficiency of a hydraulic jackhammer of a road construction machine: Dissert. of Cand. Tech. Sci., Orel, 2010. - 21 p.
- [3] Chekhutskaya N.G., Ushakov L.S. Modeling dynamic processes in a hydraulic hammer // Proc. Of the Intern. scientific. symp. "Mechanisms and machines of percussion, periodic and vibration action." - Orel: Orel State Technical University, 2000. - P. 106 - 109.
- [4] Kyzyrov K.B., Mitusov A.A., Reshetnikova O.S. Methodology of optimal designing the design parameters of hydraulic impact mechanisms: Monograph. - Karaganda: KSTU, 2019. - 123 p.
- [5] Ushakov L.C. Pulse technologies and hydraulic impact mechanisms: Textbook for universities. - Orel: Orel State Technical University, 2009. - 250 p.
- [6] Developing and studying a hydraulic impact mechanism for mining and construction works: report on research / KSTU: pr. man. K.B. Kyzyrov. - Karaganda, 2019. - 114 p. - No. GR 0118RK00681. - Inv. No. 0219RK00557.
- [7] Hydraulic hammer VKP.250. Operation manual VKP.250.00.00.000 RE. Karaganda: KSTU. - 2020. - 28 p.

Information of the authors

Kyzyrov Kayrolla Beisembaevich, candidate of technical sciences, associate professor of the department "Technological equipment, mechanical engineering and standardization" of Karaganda Technical University
E-mail: kyzyrov_k@mail.ru

Reshetnikova Olga Stanislavovna, PhD, senior lecturer of the department "Technological equipment, mechanical engineering and standardization" of Karaganda Technical University
E-mail: olga.reshetnikova.80@mail.ru

Dosmagambetov Nurlan Galymzhanovich, master student of the department "Technological equipment, mechanical engineering and standardization" of Karaganda Technical University
E-mail: dosmagambetov_n@mail.ru

Analyzing Common Transmission Mechanism of the Mining Excavator Main Mechanisms Drives

Komissarov A.P., Nabiullin R.Sh.*
Ural State Mining University, Yekaterinburg, Russia

Abstract. It has been established that with the combined action of the main mechanisms of a mining excavator in the process of excavating rocks, a common transmission mechanism for the drives of the main mechanisms is formed. It consists of a lifting mechanism, a pressure mechanism and a lever mechanism connecting the main mechanisms with a bucket. The presence of kinematic connections between the main mechanisms determines specific properties of the common transmission mechanism of the drives of the main mechanisms. It has been shown that the initial link of the common transmission mechanism, the coordinates of which determine the positions of all links of the transmission mechanism including the shafts of the engines, is the "stick-bucket" link. Based on the analysis of the common transmission mechanism, a simulation model of the excavation process with the working equipment of a straight shovel has been developed. The analytical relationships have been obtained to determine the rates of lifting and pressure, which ensure the movement of the bucket along the given trajectories in the process of working out the excavator face. The results of the work can be used in developing a control system for the main mechanisms drives of a mining excavator.

Keywords: open-pit excavator, main mechanism drives, common transmission mechanism, simulation model of the excavation process.

1. Introduction

The efficiency of the mining excavator operation is mainly determined by the degree of coordination of working movements and coordination of the work of lifting and pressure mechanisms when they act together in the process of excavating rocks.

The process of excavating rocks carried out with the coordinated work of the main mechanisms (lifting and pressure) for moving the bucket with simultaneous separation of the rock layer and with continuous change in working conditions, is difficult and limited by the psychophysical capabilities of the excavator driver. The practice of operating mining excavators shows that the duration of the working cycle in specific conditions significantly exceeds the calculated one.

In present day conditions of the market economy, the problem of increasing the efficiency of functioning the mining excavators is of particular relevance.

The known methods of determining the laws of motion of the main mechanisms are based on formal approaches: fuzzy logic, artificial intelligence, etc. [1-5].

The main trend of solving this problem is establishing the laws of motion of the main mechanisms in the process of excavation.

2. The study aim and objectives

The aim of the study is to establish the kinematic and dynamic characteristics of the excavation process by identifying the patterns of changing the operating parameters (lifting and pressure speeds) of the main mechanisms that ensure the movement of the bucket (the top of the cutting edge) along a given trajectory.

The research objectives are as follows:

- developing a mathematical model of the common transmission mechanism of the main mechanisms drives;
- determining the rates of lifting and pressure, ensuring the movement of the bucket (the top of the cutting edge) along a given trajectory.

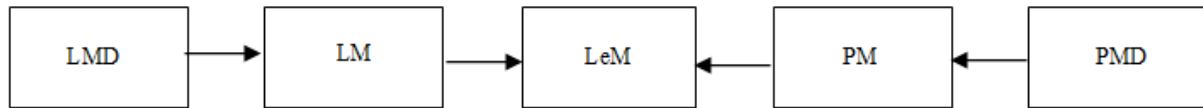
3. Solving the study objectives

The object of the research is common transmission mechanism of the main mechanisms drives.

The subject of the research is establishing functional dependencies between the parameters that determine the position of the bucket (the top of the cutting edge) in the face, and the operating parameters of the main mechanisms (lifting and pressure velocities).

The research methods are methods of the theory of machines and mechanisms, mathematical modeling and computational experiment.

In the process of excavating rocks with the combined actions of the lifting and pressure mechanisms, a common transmission mechanism of the main drives is formed (Figure 1). It consists of the main mechanisms and a linkage connecting the main mechanisms with the bucket.



LMD, PMD – drives of the lifting mechanism (LM) and pressure mechanism (PM): LeM – lever mechanism

Fig. 1. – Diagram of the common transmission mechanism of the main mechanisms drives

In this case, the main mechanisms and elements of the working equipment form a single kinematic chain, since the rack gear of the pressure mechanism is mated with the handle bar, and the hoisting rope is connected to the bucket by means of the bucket suspension rigidly fixed on the handle [6, 7].

The presence of kinematic connections between the main mechanisms determines the kinematic properties of the common transmission mechanism.

The linkage converts the motion of the main machinery into the movement of the bucket.

Lever mechanisms differ from other mechanisms in that they have “individual” kinematic properties, which are determined by the structural diagram of the mechanism, the type of kinematic connections between the links and the geometric parameters (lengths) of the links (Figure 2).

The main characteristic of the linkage is the kinematic and dynamic transfer functions (gear ratios), which determine the relationship between the kinematic and dynamic parameters of the driven and driving links [8-10].

To determine the speeds of working movements (lifting and pressure), it is necessary to set the laws of motion of the initial link, i.e., the trajectory of the bucket (the top of the cutting edge) and the digging speed, as well as the dimensions of the links of the transmission mechanism [3, 6-8].

Based on the mathematical model of the transmission mechanism, an imitation model of the process of excavation of rocks with the working equipment of the open-pit excavator has been developed, which is a set of calculated values of the operating parameters of the main mechanisms, in which the bucket moves along a given trajectory with given energy-power parameters implemented on the bucket. There have been obtained expressions for determining the speeds of the working movements (lifting and pressure), which ensure the movement of the bucket along a given trajectory.

The dependences for determining the transfer functions will be in general form:

$$\text{KTF} = \frac{V_{l(p)}}{V_b} = f_1(X_k, Y_k, l_l, l_i, \psi, \alpha_i); \quad (1)$$

$$\text{DTF} = \frac{F_{l(p)}}{F_b} = f_2(X_k, Y_k, l_l, l_i, \psi, \alpha_i, G_l, G_{lg}, F_r); \quad (2)$$

where KTF, DTF are kinematic and dynamic transfer functions;

l_l is the link length; l_i is variable link lengths (handle, bucket);

ψ is the angle of the tangent inclination to the trajectory of the bucket motion;

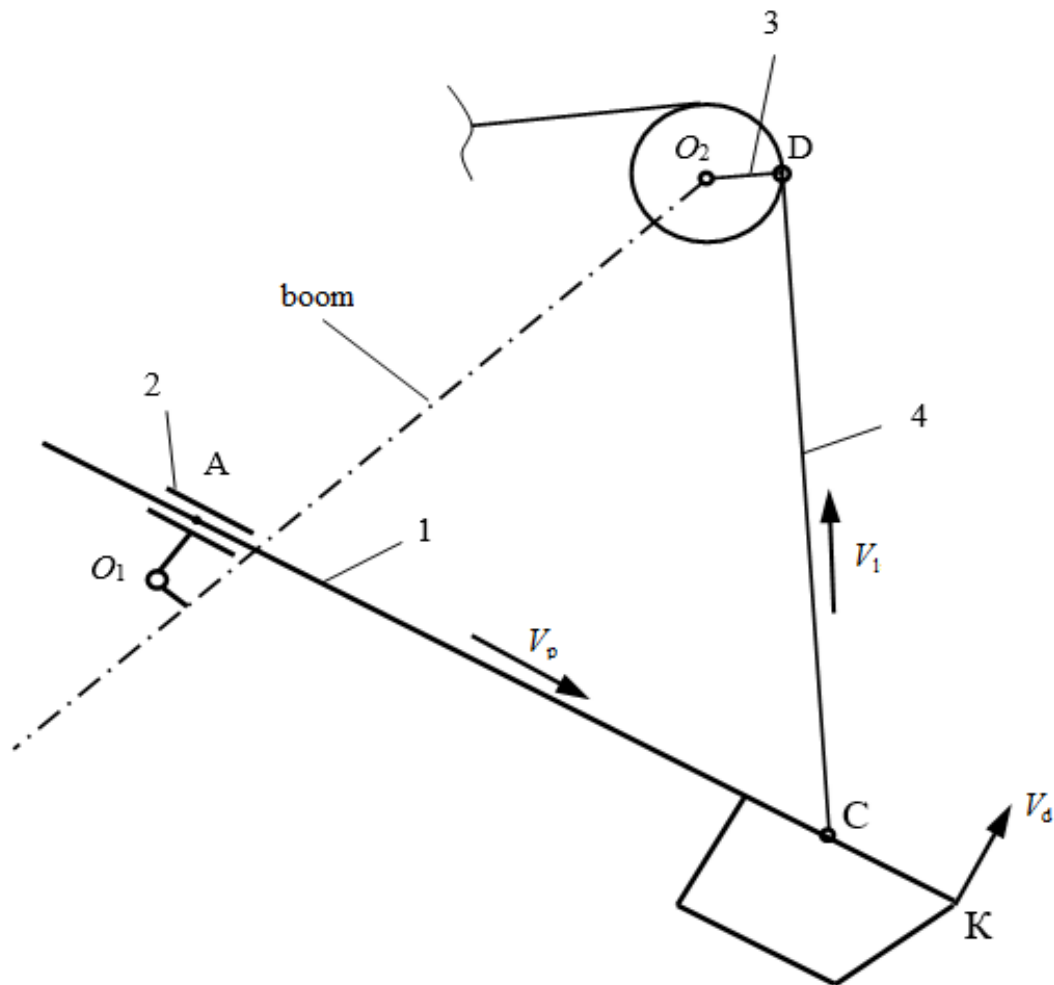
α_i is variables determining the link positions;

G_l is the link gravities;

G_{lg} is the loaded bucket gravity;

F_r is the force of digging resistance.

A computational experiment has been carried out to calculate the operating parameters of the main mechanisms of the EKG-20A excavator manufactured by the Uralmashzavod PJSC. The initial data for the calculation have been as follows: the tangential component of the digging resistance force $P_{01} = 325$ kN; the digging speed $V_b = 1$ m/s; the bucket weight $M_b = 40$ t.



1 - the "handle-bucket" link; 2, 3 - crank; 4 – lifting rope; V_d , V_1 , V_p – digging, lifting and pressure speeds

Fig. 2. – The lever mechanism diagram

The optimization algorithm for controlling the working process of a mining excavator has been developed, which ensures implementing the necessary values of the operating parameters of the main mechanisms when moving the bucket at a given digging speed within the working zone of the excavator.

The algorithm determines the content and sequence of the following operations ensuring the movement of the bucket along a given trajectory:

- computer calculating the rates of lifting and pressure in the initial position of the bucket, as well as in subsequent positions corresponding to the movement of the bucket with a given step;
- determining the values of speeds for three positions (initial, middle and final) and transmission of commands proportional to the values of speeds to the input of the control system of the main mechanisms drives;
- moving the bucket to the next position.

The simulation model of the excavation process determines the digital control algorithm, which forms a control action on the main mechanisms drives.

Thus, on the basis of a simulation model of the excavation process obtained as a result of the computational experiment, it is possible to determine for any point in the working area of the excavator the operating parameters of the main mechanisms at the given power parameters implemented on the bucket and for a given trajectory of the bucket movement (the top of the cutting edge).

3. Conclusions

The proposed method of calculating the operating parameters (lifting and pressure rates) of the main mechanisms of open pit excavators by means of a computational experiment makes it possible to determine the actual values of the speeds of working movements in specific mining conditions (the face dimensions, the type of bucket trajectories, etc.).

Establishing the interdependences between the operating parameters of the main mechanisms during excavation can serve as the basis for the development of an adaptive system of digital control of the main mechanisms drives, which, due

to the coordination of the speeds of working movements in specific operating conditions, increases the efficiency of the excavator.

4. References

- [1] Babakov S.E., Pevzner L.D. Algorithmization of controlling the excavator bucket movement in the digging mode with the use of fuzzy logic// Mining equipment and electromechanics, № 9, 2012. - P. 8 - 17.
- [2] Koryukov A.A. Geometric model of the working equipment of a quarry excavator for calculating the loads of the electric drive and monitoring the position of the bucket// Izvestiya vuzov. Mining Journal. 2013, N. 3. - P. 106 - 113.
- [3] Malafeyev S.I. Intellectualization of a quarry excavator // Mining information and analytical bulletin, N 11, 2015, - P. 107 - 115.
- [4] Pevzner L.D. Automated control of powerful single-bucket excavators. - M.: Mining, 2014. - 400 p.
- [5] Pevzner L.D., Babakov S.E. Algorithm of managing the operation of digging an open-pit excavator-shovel with the use of fuzzy logic// Mining information-analytical bulletin, № 1, 2015. - P. 263 - 271.
- [6] Gafuryanov R.G., Komissarov A.P., Shestakov V.S. Modeling of the working process of open pit excavators. Mining equipment and electromechanics. 2009. № 6. - P. 40 - 45.
- [7] Komissarov A.P., Letnev K.Yu., Lukashuk O.A. Analysis of double-crank-lever mechanisms of working equipment of open-pit excavators. Technological equipment for mining and oil and gas industry: collection of works. works XIV Intern. scientific and technical conf. "Readings in memory of V.R. Kubachek". Yekaterinburg (April 20-21, 2017): USMU Publishing House, 2017. - P. 41 - 46.
- [8] Lukashuk O.A., Letnev K.Yu., Komissarov A.P. Determining the operating modes of engines of the main mechanisms of a single-bucket excavator// Izvestiya. vuzov. Mining Journal, № 5. 2017. - P. 52-58.
- [9] Levitsky N.I. Theory of mechanisms and machines. - M.: Nauka, 1979. - 576 p.
- [10] Malafeyev S.I., Tikhonov Yu.V. Intelligent control components for mining excavators //Automation in industry, № 10, 2013. - P. 33 - 37.
- [11] Poderny R. Yu. Mechanical equipment for quarries. 6th ed., rev. and add. - M.: MSMU, 2007. - 680 p.

Information of the authors

Komissarov Anatoly Pavlovich, doctor of technical sciences, professor of the department "Handling Machines and Robots", Ural State Mining University

E-mail: komissarov_a_p@mail.ru

Nabiullin Rustem Shafkatovich, candidate of technical sciences, associate professor of the department "Mining Machines and Complexes" of Ural State Mining University

E-mail: nabiullin.r@m.ursmu.ru

Studying Gamma-albedo Method Sensitivity to Control Effective Atomic Number of Complex Materials

Pak Yu.N.* , Pak D.Yu., Tebayeva A.Yu., Malikov N.M
Karaganda Technical University, Karaganda, Kazakhstan
*corresponding author

Abstract. A mathematical model of the gamma-albedo method is proposed to control the effective atomic number Z of complex materials. An analytical expression for calculating the sensitivity to Z has been obtained. It has been shown that the method sensitivity is a complex function of the primary gamma radiation the energy and the Z value of the material. The inversion character of the dependence of the method sensitivity on the effective atomic number has been established. The maximum sensitivity naturally shifts to the region of increased Z values with increasing the primary gamma radiation energy. The satisfactory convergence of the calculated and experimental values of the sensitivity indicates suitability of the mathematical model for optimizing the parameters of the method for controlling the material Z .

Keywords: *gamma-albedo method, effective atomic number, scattered gamma radiation, method sensitivity, optimizing the parameters.*

1. Introduction

When controlling the quality of complex materials, it is important to achieve increased differentiation of the results of the method to changing the effective atomic number (elemental-chemical composition) of complex materials and substances. The main metrological parameter that determines the methodological capabilities of any physical (instrumental) method is the relative sensitivity (contrast), which characterizes the relative dN/N increment of the measured instrumental signal N for a single dZ changing in the effective atomic number Z of a complex material:

$$S = \frac{dN}{NdZ} \quad (1)$$

The information of sensitivity allows optimizing the parameters of any instrumental method in terms of achieving the maximum accuracy in determining the effective atomic number under the influence of disturbing factors.

Various modifications of the gamma-albedo method based on irradiation of the studied material with a flux of gamma radiation and registration of the gamma radiation scattered by it, have become widely used in the practice of quality control of various materials, substances and products [1 - 4]. These modifications of the gamma-albedo method implemented with different energies of primary and scattered gamma radiation and measurement geometry (a primary gamma radiation source – a control object – a scattered radiation detector) are aimed at solving the problem of material quality control based on the relationship between the effective atomic number \bar{Z} of materials and the content of individual elements, as well as between \bar{Z} and the density of materials. It is obvious that for a priori assessment of the method sensitivity according to expression (1), a mathematical model is needed that describes the dependence of the measured signal (the intensity of gamma radiation scattered by the material) on the gamma-attenuating characteristics of the materials under study.

2. Mathematical model

Theoretical substantiation of the gamma-albedo method has been performed in the approximation of a point monochromatic source of gamma radiation and an isotope detector located at a finite distance from one another and remote from the surface of the material under study at the distance H . Such an approximation corresponds to real conditions in studying various materials by nuclear physical methods [3]. The dependence of the intensity of scattered gamma radiation on the effective atomic number of a complex material and other influencing factors can be described by the method of statistical modeling (Monte Carlo) based on the approximation of the true physical processes of interaction of gamma radiation by some numerical models [5]. The method has been used limitedly in gamma albedo practice so far. To describe the albedo of gamma radiation, the analytical expression was used obtained in the approximation of a single interaction for a zero probe:

$$\mu = kN_0\sigma[H^2(\mu_0 + \mu_S)]^{-1}, \quad (2)$$

where N_S is the density of the scattered by the material gamma radiation flux;

N_0 is the density of the primary gamma radiation flux;

k is a constant factor dependent on the measurement geometry;

σ is the mass scattering coefficient of the primary radiation by the material;

μ_0, μ_S is the mass attenuation coefficient of the primary and scattered radiation by the material, respectively.

For gamma radiation with energies below ~ 500 keV, attenuation of the primary and scattered radiation is mainly determined by two processes: Compton scattering and photoelectric absorption. The dependence of the mass attenuation coefficient on the energy of gamma radiation and the atomic number Z is determined by the following empirical (for photoelectric absorption) and exact (for Compton scattering) expressions [5]:

$$\begin{aligned}\mu_f &= 15,2m(Z^3/E^3); \\ \mu_k &= \pi r_0^2 N_A m f(a).\end{aligned}\quad (3)$$

where $m = 2Z/A$ is the electronic density coefficient;

A is the element mass number;

r_0 is the electron classic radius;

N_A is the Avogadro number;

$$f(a) = \frac{a^2 - 2a - 2}{2a^2} \ln(1 + 2a) + \frac{a^3 + 9a^2 + 8a + 2}{a^2(1 + 2a)^2};$$

$$a = \frac{E}{511}.$$

After simple transformations taking into account the coefficient m proximity to 1, expression (3) can be reduced to the form:

$$\begin{aligned}\mu_f &= 15,2Z^3/E^3; \\ \mu_k &= 0,15 f(a).\end{aligned}\quad (4)$$

Taking into account expression (4) and the Compton formula for scattered gamma radiation, as well as the independence of the mass scattering coefficient σ on Z within the approximate equality ($m \approx 1$), the flux density of scattered gamma quanta depending on the effective atomic number of a complex material, can be expressed in the form:

$$N_S = \frac{K_1}{15,2Z^3[(E_0^3)^{-1} + (E_S^3)^{-1}] + 0,15[f(a_0) + f(a_S)]}, \quad (5)$$

where $K_1 = KN_0\sigma/H^2$; $a_0 = E_0/511$; $a_S = E_S/511$.

Differentiating expression (5) on dZ according to (1), we obtain an analytical relationship for calculating the method relative sensitivity to the effective atomic number:

$$S = - \frac{45,6Z^2[(E_0^3)^{-1} + (E_S^3)^{-1}]}{15,2Z^3[(E_0^3)^{-1} + (E_S^3)^{-1}] + 0,15[f(a_0) + f(a_S)]} \quad (6)$$

3. Results of the studies

The computational studies have shown that the contrast of the gamma-albedo method is a complex function of the applied gamma radiation the energy and the effective atomic number of the analyzed materials (Figure 1). With increasing the radiation energy, a regular decrease in the sensitivity to Z is observed. For light materials (Z is small), the sensitivity gradient S in the low-energy region is higher. For heavier elements (Z is greater), a smoother decrease in S is observed depending on energy.

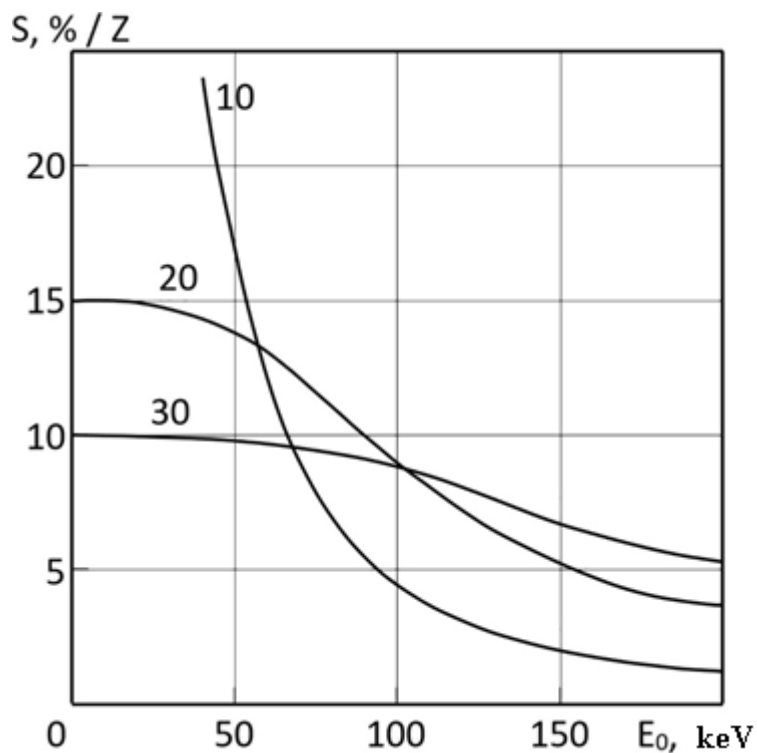
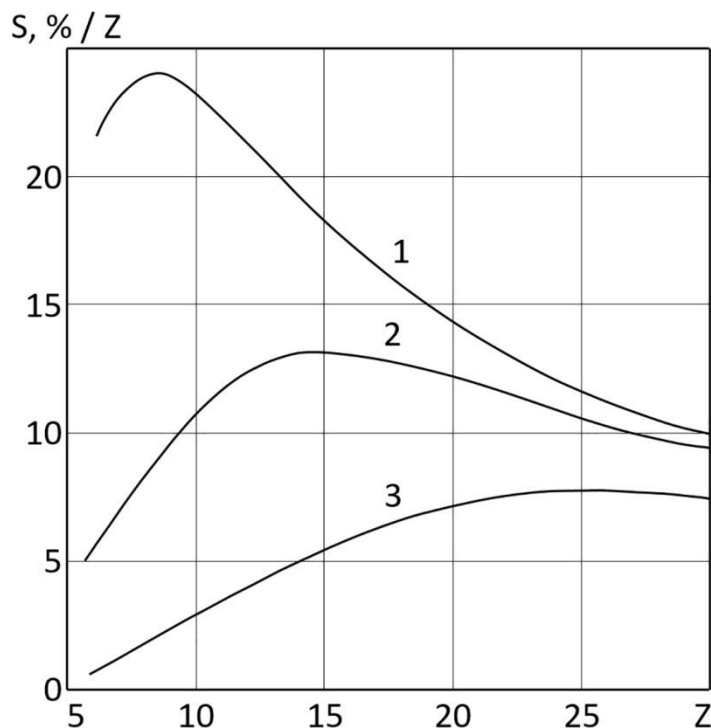


Fig. 1. – Relative sensitivity to Z dependence on the primary γ - radiation energy
The curvature code is the Z value

The inversion character of the sensitivity S dependence on the value of the effective atomic number of the material seems to be interesting (Figure 2). The maximum sensitivity naturally shifts to the region of increased Z values with increasing energy of the primary gamma radiation.



1 – 30 keV; 2 - 60 keV; 3 - 120 keV

Fig. 2. – Relative sensitivity to Z dependence on the effective atomic number of the material with the primary gamma radiation energy

Using expression (6), it is not difficult to obtain an analytical relationship that determines the position of the sensitivity dependence maximum to the atomic number on the Z scale:

$$Z_i = \frac{\sqrt[3]{0,02[f(a_0)+f(a_S)]}}{[(E_0^3)^{-1}+(E_S^3)^{-1}]} \quad (7)$$

The obtained relationship allows optimizing the selection of the primary gamma radiation energy in terms of achieving the maximum contrast of the gamma-albedo method in the real range of the effective atomic number of complex materials. The Table below presents comparative data of the gamma-albedo method sensitivity to the effective atomic number of various materials for $E_0 = 60$ keV.

Table 1 – Comparison of the calculated and experimental data of the sensitivity to Z

Material – alloy Z	Sensitivity, percent/ Z		Relative divergence, %
	calculation	experiment	
Graphite 6	6.1	5.7	6.5
Alloy Al 13,3	13.2	12.1	8.3
Alloy Fe – Mn 25,9	10.1	9.4	7.0

The satisfactory convergence of the calculated and experimental data of the sensitivity to Z indicates suitability of the mathematical model for assessing the metrological characteristics of the gamma-albedo method, in particular, for determining impurity elements in materials of quasi-binary composition.

4. Conclusions

Based on the proposed mathematical model of the gamma-albedo method, an analytical expression has been obtained to assess the sensitivity to the effective atomic number of materials. Computational studies have revealed dependences of the method sensitivity to Z on the energy of primary gamma radiation and the value of Z. A relationship has been found that allows optimizing the parameters of the method (selecting energy, the real interval of the Z value) in terms of achieving the maximum sensitivity of the method for controlling Z of complex materials.

5. References

- [1] Bulatov B.P., Andryushin N.F. Backscattered gamma radiation in radiation technology. - M.: Atomizdat, 1975. - 240 p.
- [2] Klyuev V.M., Yermolov I.N., Mayorov A.N., et al. Instruments for non-destructive testing of materials and products / Ed. V.M. Klyuev. M.: Mashinostroenie, 1976. - 741 p.
- [3] Pak Yu.N., Pak D.Yu. Nuclear technologies in geophysical research. Karaganda: KSTU Publ. House, 2016. - 346 p.
- [4] Chudakov V.A., Anshakov O.M. Radioisotope measurement of the light media density. Minsk: BSU Publ. House, 1982. - p. 141.
- [5] Pshenichny G.A. Interaction of gamma radiation with matter and modeling of problems in nuclear geophysics. - M.: Energoizdat, 1982. - 224 p.

Information of the authors

Pak Yuriy Nikolaevich, doctor of technical sciences, professor of the department "Development of mineral deposits" of the Karaganda Technical University

E-mail: pak_gos@mail.ru

Pak Dmitry Yurievich, candidate of technical sciences., Professor of the Department "Development of mineral deposits" of the Karaganda Technical University

E-mail: pak_kargtu@mail.ru

Tebaeva Anar Yulaevna, master, assistant of the department "Development of mineral deposits" of the Karaganda Technical University

E-mail: tebaeva_a@mail.ru

Malikov Nurbol Muratovich, master, lecturer at the department "Energy systems", Karaganda Technical University

E-mail: malikov_n@mail.ru

Development of a Mathematical Model of a Device for Cleaning Road Surfaces from Ice

Gavrilin A.N.*

Tomsk Polytechnic University, Tomsk, Russia

*corresponding author

Abstract. A variant of a combined schematic diagram of a device for cleaning road surfaces from ice is proposed. The developed design of the device for cleaning road surfaces from ice is also shown. The principle of operation of a structure with an adjustable oscillator is described. In accordance with the block diagram, a design diagram and a mathematical model of the dynamic interaction of the oscillatory circuit and the vehicle have been drawn up. The effectiveness of the developed device is determined by an increase in the productivity and quality of road cleaning from ice.

Key words: vibration, vibration generator, vibrator, road cleaning, device dynamics.

1. Introduction

One of the main causes of road accidents in the winter period is the unsatisfactory quality of the road surface. At the same time, a significant part of road accidents occurs due to the low coefficient of adhesion of the road surface to the wheels of cars, that is, due to slipperiness.

Currently, there are several known ways to combat winter slipperiness of road surfaces, the most common can be divided into two groups: a mechanical method of cleaning road surfaces and a method using anti-icing materials [1].

The method using anti-icing materials is the most common not only in the Tomsk region, but also in the country as a whole. However, it is not environmentally friendly and ineffective at temperatures below minus 25 °C [2].

The mechanical method of cleaning road surfaces from ice is environmentally friendly and effective at temperatures below minus 25 °C.

In connection with the above factors, the development and research of devices for cleaning road surfaces from ice is a topical topic. The study of dynamics is aimed at reducing the magnitude of dynamic effects on the vehicle carrying out mechanical processing (together with the operator) by achieving optimal parameters of the device.

The problem in this case is insufficient cleaning of the road surface from ice in winter at sufficiently low air temperatures, especially on steep slopes. Therefore, the solution to this problem by creating a device for cleaning road surfaces from ice with a shearing tool is relevant.

The invention relates to municipal engineering for cleaning road surfaces from ice.

2. Results and discussion

2.1 Device design

Examination of patent inventions showed that the device with a vibration shear load is a modern development.

This is justified by the low energy consumption, as well as the ability to regulate the cleavage depth by changing the amplitude [3]. Taking into account the shortcomings of existing technical solutions, it is necessary to develop a fundamentally new device for cleaning road surfaces from ice, by means of design refinement, to improve the quality and productivity of cleaning. Investigate the possibilities of regulating the amplitude of movement of the shearing tool of the new device by selecting the resonance mode. All of the above indicates the relevance of this study.

A combined device is proposed with the addition of a hydraulic vibrator on elastic shells between the fixed and movable frames of the shearing tool.

Boundary conditions of the research object:

- the thickness of the road ice - from 0 to 200 mm;
- the maximum frequency of rotation of the oscillation generator - up to 4000 rpm.

The developed design of the device for cleaning road surfaces from ice is shown in Figure 1. The device is designed to ensure the safe movement of vehicles and pedestrians by increasing the coefficient of adhesion of tires to the road surface, ie. by changing the roughness of the road surface by means of mechanical cleaning.

The device (Fig. 1) has a main frame 4, pivotally connected to the vehicle 12, contains a retainer 13. A beam 2 is attached to the main frame 4 by means of a hinge, on which a mechanism for adjusting 14 the length of the load arm is installed 3. Beam 2 is connected to a shear wheel 1 using plain bearings. Shear wheel 1, movable beam 2 with load 3 and control mechanism 14 constitute an oscillatory circuit (OC), which is pivotally connected to the main frame 4 [4].

The shear wheel 1 is a disc with teeth on its outer circumference. Spacers 6 and high pressure hoses (HPH) 5 are installed between the main frame 4 and the beam 2.

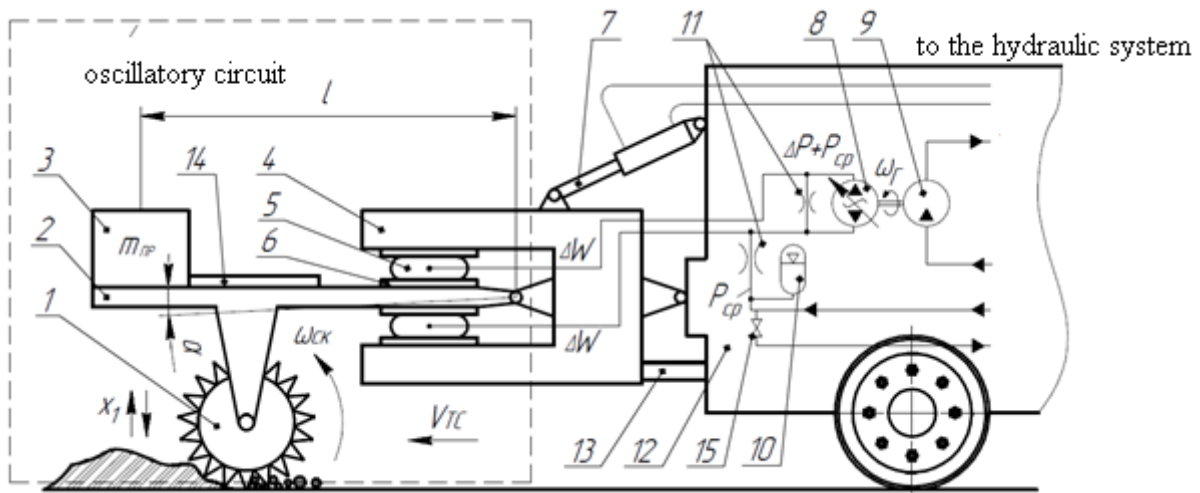


Fig. 1. - Schematic diagram of a device for cleaning road surfaces from ice

The device is driven from the vehicle's hydraulic system using additional built-in hydraulic units: hydraulic pump, hydraulic motor 9, powered by the vehicle's hydraulic system; an adjustable oscillation generator 8, connected by a hydraulic line with a high pressure arm 5 (HPR). Elastic shells 5 (HPR) between the fixed main frame of the device 4 and the movable beam 2 form a hydraulic vibrator.

To maintain the average pressure P_{cp} in the hydraulic system, a hydraulic accumulator 10 and nozzles 11 are used. At the end of the work, opening the valve 15 is used to drain the hydraulic oil into the hydraulic system of the vehicle.

To prevent accidents, safety valves (not shown in the diagram) are installed in the hydraulic system of the device. The kinematic and hydraulic diagram of the device for cleaning road surfaces from ice is shown in Figure 2.

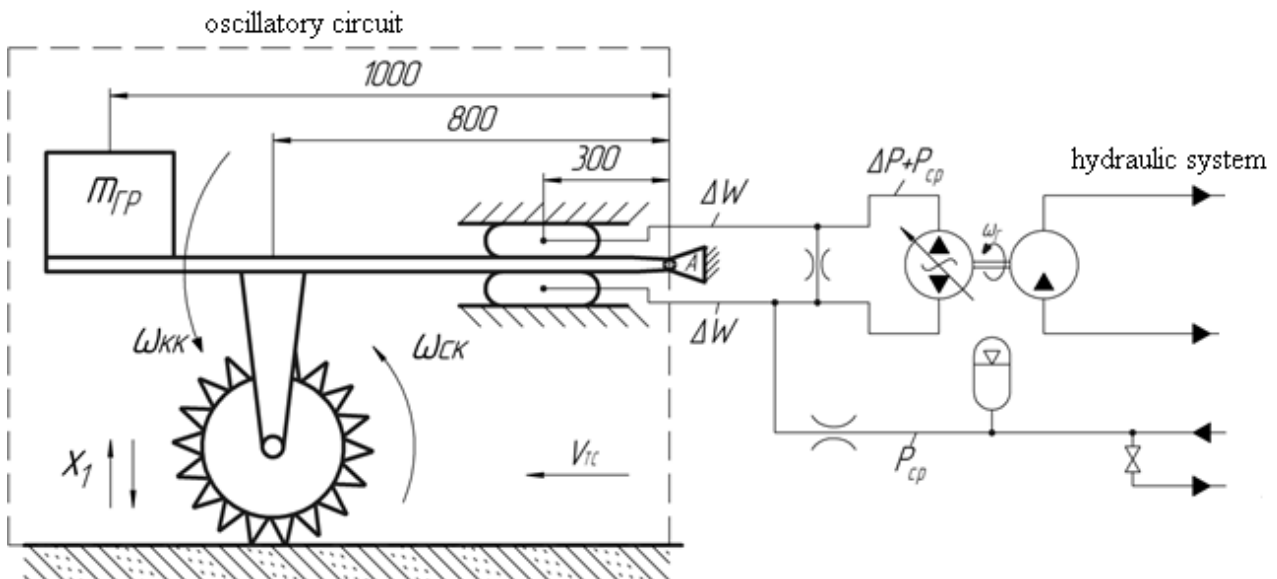


Fig. 2. - Combined scheme (kinematic and hydraulic) device for cleaning road surfaces from ice

The device works (Fig. 1) as follows. The vehicle with the device is installed on a snow-covered or icy section of the road surface. The operator, using the hydraulic cylinder 7, lowers the frame 4 until the shear wheel 1 comes into contact with the ice. After installing the device on the road surface, the operator turns on the lock 13, thereby the main frame 4 becomes rigidly fixed to the vehicle 12. The hydraulic motor 9 rotates an adjustable oscillation generator 8 (Fig. 3), which creates a pulsating volume of the working fluid according to a law close to harmonic (WA - the amplitude value of the pulsating volume).

The pulsating volume of the working fluid $\Delta W(t)$, entering the high-pressure hose 5, previously deformed in the radial direction (vibrator), generates the force F_6 and the corresponding vibration displacement of the movable beam 2 and the shear wheel 1. The operator sets the vehicle in motion, which moves at a certain speed V_{TC} . As a result of the vibration impact of the shear wheel 1, ice from the road surface is destroyed [5].

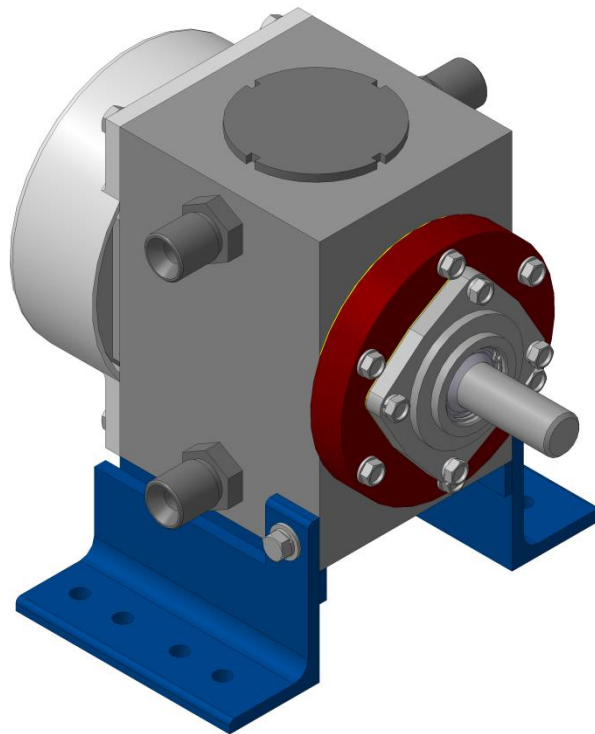


Fig. 3. - Adjustable oscillator

The thickness (amplitude of the OC oscillations) of the destruction of ice is regulated by the kinetic energy of vibration of the oscillatory circuit of the device. The amplitude of the oscillatory circuit can be adjusted by changing the excitation frequency of the generator ωG , which, when it coincides with the resonant frequency of the OC, will be maximum (formula 1).

It should be noted that the device allows you to adjust the kinetic energy for the destruction of ice, depending on the thickness of the sheared layer, by changing the following parameters: the length of the arm l of the movable weight, as well as the value of the pulsating volume, which directly affects the value of the pulsating pressure.

A test sample was developed with the support of the Western Siberia Corporation LLC (Tomsk) (Fig. 4). Preliminary tests of the device operability, carried out at the enterprise, showed good results.

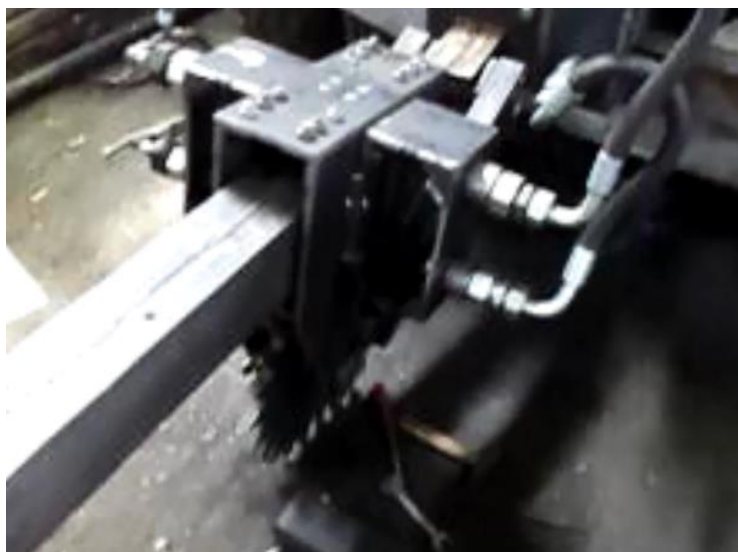


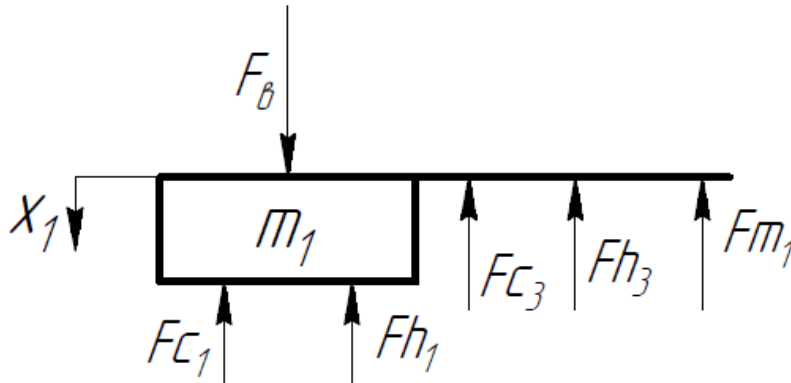
Fig. 4. - Prototype device for cleaning road surfaces from ice

2.2 Development of a mathematical model of the device

The need to consider the mathematical model of the device is due to the fact that the results obtained will optimize the parameters of the device, thereby improving the quality and productivity of cleaning the road surface from ice [6]. The model assumes that the road ice has the same thickness.

The development of a mathematical model is possible only after solving the design scheme. The solution of the design scheme of the device is carried out using a detailed analysis of each subsystem. It is necessary to consider separately the design scheme of the oscillatory circuit and the vehicle. Next, arrange the forces acting on each subsystem. Consider the analysis of the action of forces with an oscillatory circuit that has a mass m_1 .

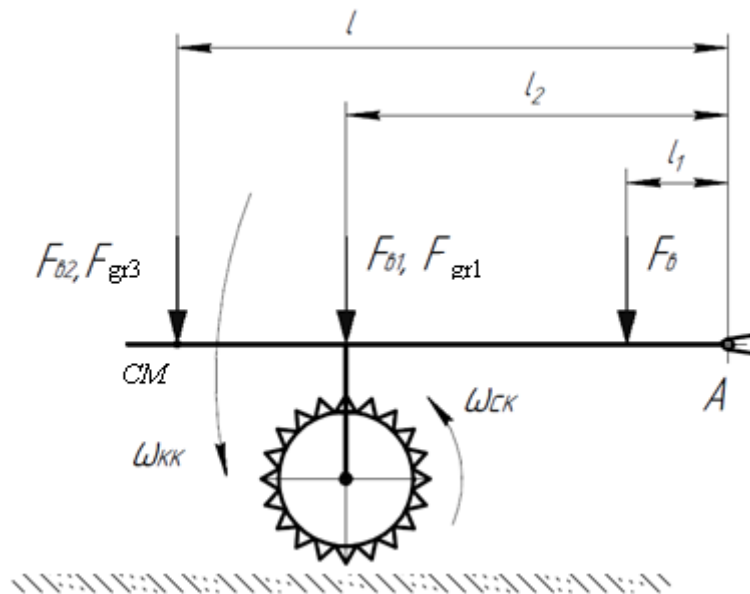
Consider the analysis of the action of forces F_B with an oscillatory circuit that has a mass (Figure 5).



F_{m1} – force of inertia OC; F_{h1} , F_{h3} – respectively, the damping forces of ice and high-pressure hoses; F_{c1} , F_{c3} – respectively the force of rigidity of ice and high pressure hoses

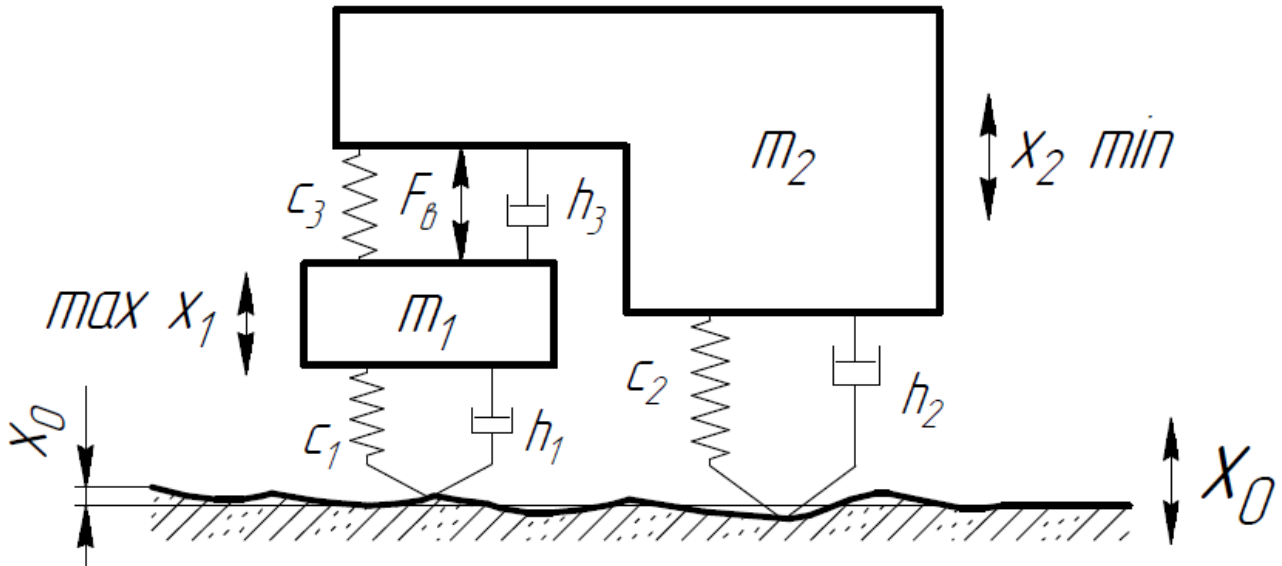
Fig. 5. - Design diagram of the forces acting on the oscillatory circuit

The design diagrams of the acting forces on the oscillatory one are presented in Figures 6 and 7.



CM – center of mass; ω_{CK} , ω_{KK} – respectively, the angular frequency of the shear wheel and the oscillatory circuit; l_1 , l_2 , l_3 – respectively, the length of the arm of the high-pressure sleeve, shear wheel and center of mass; F_B – external force of the vibrator generated by the oscillator; F_{B1} – vibrator force on shear wheel, F_{B2} – vibrator force applied to the center of mass; F_{gr1} , F_{gr3} – respectively, the force of gravity of the shear wheel, the center of mass.

Fig. 6. - Kinematic design diagram of the oscillatory circuit



m_1 – reduced mass of the oscillating circuit; m_2 – reduced vehicle mass; c_1, c_2, c_3 – respectively, the reduced coefficients of elasticity of ice, vehicle, high-pressure hoses; h_1, h_2, h_3 – respectively, the reduced damping coefficients of ice, vehicle, high-pressure hoses; F_b – external force of the vibrator generated by the oscillator; x_0, x_1, x_2 – accordingly, the movement caused by the unevenness of the road surface, masse m_1 и m_2

Fig.7. - Design diagram of a device for cleaning road surfaces from ice

Based on the design diagram of the acting forces on the oscillatory circuit (Fig. 6, 7), the equation of the balance of forces for the oscillatory circuit:

$$F_{\theta_1} = Fm_1 + Fh_1 + Fh_3 + Fc_1 + Fc_3 \quad (1)$$

The external force of the vibrator F_{θ} changes according to the sine law, therefore, it is determined by the formula:

$$F_{\theta}(t) = F_A \cdot \sin(\omega t + \psi_0) \quad (2)$$

where F_A - amplitude force of the vibrator, N;

ω – vibrator excitation frequency, rad / s;

t – время, с;

ψ_0 - phase, rad / s.

The amplitude force of the vibrator F_A is determined by the following formula:

$$F_A = P_{\max} \cdot S \quad (3)$$

where P_{\max} - maximum pressure in the sleeve, Pa;

S – active contact area of the high-pressure hose, m^2 .

According to the diagram of the distribution of forces on the beam (Fig. 6), the force of the vibrator on the shear wheel is determined by correcting the ratio of the levers l_1 to l_2 . Then the external force on the shear wheel is determined by the formula:

$$F_{\theta_1} = \frac{F_{\theta} \cdot l_1}{l_2} \quad (4)$$

The force of inertia of the shear wheel is determined by the formula:

$$Fm_1 = \frac{F_{un3} \cdot l}{l_2} \quad (5)$$

The force of inertia of the center of mass of the oscillatory circuit is determined by the formula:

$$F_{un3} = m_1 a_1 \quad (6)$$

where a_1 - acceleration of the center of mass of the oscillating circuit, m / s^2 .

The force of inertia of the shear wheel, taking into account equation (6), is determined by the formula:

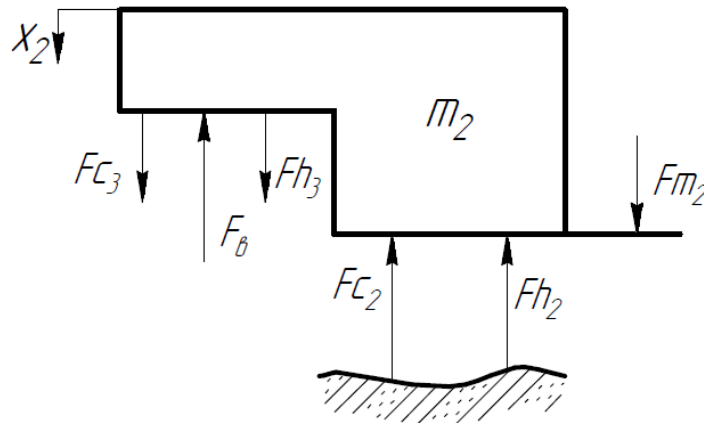
$$Fm_1 = \frac{m_1 a_1 \cdot l}{l_2} \quad (7)$$

We replace $F_{\theta 1}$, Fm_1 , Fh_1 , Fc_1 , Fc_3 , Fh_3 in equation (1), then we obtain a complete equation that describes the motion of the oscillatory circuit depending on time:

$$P_{\max} S \frac{l_1}{l_2} \sin(\omega t + \psi_0) = m_1 a_1 \frac{l}{l_2} + h_1(v_0 - v_1) + h_3(v_1 - v_2) + c_1(x_0 - x_1) + c_3(x_1 - x_2) \quad (8)$$

Consider the design diagram of the forces acting on the vehicle (Fig. 8). Vibrations of the vehicle in the vertical direction occur under the action of the forces of stiffness Fc_2 and damping Fh_2 , they are external forces for the vehicle.

The vehicle is influenced by the force of the vibrator F_{θ} , which is counteracted by the forces of stiffness and damping.



Fm_2 - the force of inertia of the vehicle; Fh_2 - damping force of the vehicle wheels; Fc_2 - the force of rigidity of the wheels of the vehicle

Fig. 8. - Design diagram of the forces acting on the vehicle

Based on the design diagram of the forces acting on the vehicle (Fig. 8), the equation for the balance of forces for the vehicle:

$$F_{\theta} + Fc_2 + Fh_2 = Fm_2 + Fh_3 + Fc_3 \quad (9)$$

We replace F_{θ} , Fc_2 , Fh_2 , Fm_2 , Fc_3 , Fh_3 in equation (9), then we get an equation that describes the movement of the vehicle depending on time:

$$P_{\max} \cdot S \cdot \sin(\omega t + \psi_0) + c_2(x_0 - x_2) + h_2(v_0 - v_2) = m_2 a_2 + h_3(v_1 - v_2) + c_3(x_1 - x_2) \quad (10)$$

The mathematical model of the device for cleaning road surfaces from ice consists of: the equation of the oscillatory circuit (8) and the equation of the vehicle (10):

$$\left\{ \begin{array}{l} \frac{dx_1}{dt} = v_1; \\ \frac{dv_1}{dt} = \frac{l_2 \cdot (P_{\max} S \frac{l_1}{l_2} \sin(\omega t + \psi_0) - h_1(v_0 - v_1) - h_3(v_1 - v_2) - c_1(x_0 - x_1) - c_3(x_1 - x_2))}{l \cdot m_1}; \\ \frac{dx_2}{dt} = v_2; \\ \frac{dv_2}{dt} = \frac{P_{\max} \cdot S \cdot \sin(\omega t + \psi_0) + c_2(x_0 - x_2) + h_2(v_0 - v_2) - h_3(v_1 - v_2) - c_3(x_1 - x_2)}{m_2}; \end{array} \right. \quad (11)$$

The mathematical model of the device is represented by the system of equations (11), taking into account the methods considered in [7, 8], which makes it possible to assess the amplitude of movement and the speed of the amplitude of oscillations and the vehicle for operation in optimal modes. You can use the obtained speed value from equation (11) to determine the kinetic energy of the oscillating circuit and the vehicle.

3. Conclusions

1) As a result of the analysis of mechanical devices for cleaning road surfaces from ice, a schematic diagram of a new device for cleaning road surfaces from ice was developed. The proposed design has low energy consumption and sufficient performance.

2) On the basis of the schematic diagram of the device, a block diagram has been drawn up, which includes three subsystems: a hydraulic drive, an oscillatory circuit and a vehicle.

3) In accordance with the block diagram, a design scheme for the interaction of two subsystems was drawn up: an oscillatory circuit and a vehicle. On the basis of the design scheme, a mathematical model has been drawn up, which allows taking into account the mutual energy exchange between the amplitude of the oscillations and the vehicle.

4. References

- [1] Dudkin M. V., Fadeyev S. N., Pichugin S. YU. Metodika razrusheniya ledyanogo pokrytiya na avtomobil'nykh dorogakh rabochim organom udarnogo deystviya // *Novosti nauki Kazakhstana*. № 3(125), 2015. – P. 177 – 191.
- [2] Podol'skiy V.P., Samodurova T.V. *Ekologiya zimnego soderzhaniya avtomobil'nykh dorog*. - M.: Informavtodor, 2003. - 96 p.
- [3] Bondarenko V.A., Frolova D.S., Shcherba Ye.M. Modelirovaniye vibratsionnogo vozdeystviya pri dvizhenii transportnykh mashin v usloviyakh promyshlennykh predpriyatii // *Internet-zhurnal «Naukovedeniye»*, Tom 9, №5, 2017. – P.1 - 11
- [4] Kravchenko V.A. Agregat ochistki ot naledi i spressovannogo snega. Rossiyskiy patent. 27.01.2007
- [5] Ayupov V.V. Matematicheskoye modelirovaniye tekhnicheskikh sistem: uchebnoye posobiye. - Perm': IPTS «Prokrost», 2017 – 242 p.
- [6] Bal'va O.P. *Fizika*. Universal'nyy spravochnik. - M.: Yauza–press, 2013. - 320 p.
- [7] Ivanov S.Ye., Gavrilin A.N., Kozyrev A.N., Moyzes B.B. Povysheniye effektivnosti frezernoy obrabotki putom snizheniya udarno-vibratsionnykh nagruzok // *Polzunovskiy vestnik*, № 1, 2018. – P. 77 - 81.
- [8] Mikishanina E A. Mathematical modeling of multilayer road surfaces // *IOP Conference Series Earth and Environmental Science*, January 2020. - P. 1 – 8.

Information of the authors

Gavrilin Aleksey Nikolaevich, doctor of technical sciences, professor of mechanical engineering department of Tomsk polytechnic university
E-mail: gawral@tpu.ru

Research of the Process of Obtaining Blanks by Combining Casting and Heading

Bukanov Zh.U.*

Karaganda Technical University, Karaganda, Kazakhstan

*corresponding author

Abstract. The article discusses a new method of producing products by combining casting and extrusion. The results of the study of the process are presented. Determination of technological and kinematic parameters of the process of combining casting and heading. Calculation of the cooling time of liquid metal in a water-cooled crystallizer.

Keywords. crystallizer, casting, heading, cooling, liquid metal.

1. Introduction

Increasing process productivity, product quality, reducing energy costs and material consumption has always been one of the priority areas for developing the potential of any country. One of the ways for successful development, in particular, in metallurgy and mechanical engineering, are methods that combine continuous casting and pressure treatment. For example, the production of continuously cast slabs and blanks, modern casting and rolling modules and methods of metal processing, which ensure an increase in the quality and productivity of the process. Therefore, the method that combines the casting of blanks with subsequent plastic processing is one of the most effective methods that favorably affects the formation of an optimal internal structure and an increase in labor productivity. Metal processing processes are used not only to give certain sizes and shapes, but also to achieve a given set of properties. In addition to changing the geometry of a deformed object, the main task of metal processing is to ensure significant structural changes that determine a significant increase in physical and mechanical properties, as well as an increase in the productivity of the process.

Therefore, the development of a new method that combines casting of blanks with subsequent extrusion to obtain a finished part is of great interest among specialists involved in the creation of new materials with improved mechanical properties and ultrafine-grained structure.

In addition, of great interest are the basic laws and phenomena that occur during the implementation of a new method that combine the processes of casting and subsequent extrusion. For example, as a quality change of the metal, the structure and properties of the metal extrusion force. All these new data obtained will significantly supplement the scientific stock and significantly increase the scientific potential of any country.

One of the main tasks in this work is the determination and construction of temperature fields during cooling of cast blanks in a crystallizer, the mechanism of solidification of liquid metal and the gradual squeezing of a "healthy" crust into the open cavity of the matrix, the effect of plastic deformation on the structure and properties of the resulting metal products.

2. Results and discussion

In this case, the technological parameter should mainly mean the above-mentioned solidification time of liquid metal t_{cr} , although the technological parameters are the degree of deformation of the workpiece ε , the processing temperature $T^{\circ}C$ and others, which significantly affect the degree of filling of the matrix. If the temperature $T^{\circ}C$ is too low, then the matrix cavity will be difficult to fill, and vice versa, if it is too high, then it will be filled with liquid metal, as in injection molding. In addition, when in a semi-liquid state, the quality of the metal will be poor, and a loose structure will form. Therefore, the difficulty lies in creating the following condition:

$t_{crank} \approx t_{cr}$, where t_{crank} – the time of movement of the main units of the machine, i.e. slider and matrix, t_{cr} – time of crystallization of liquid metal in the mold.

The consistency of the specified time values should ensure, at the end of the process, the receipt of solidified high-quality metal products.

To determine the cooling time of the liquid metal, it is necessary to construct the temperature fields when it is cooled in the mold. It should be noted that the set of temperature values at a given time is called the temperature field. Temperature T is a function of coordinates ρ , θ , z and time t , if we take a cylindrical coordinate system when cooling a metal in a circular mold, i.e. $T = \varphi(\rho, \theta, z, t)$ [1-3].

If the temperature is a function of three coordinates, then such a field is called three-dimensional. If the temperature is a function of two coordinates, then the temperature field is called two-dimensional, and if the temperature is a function of one coordinate, for example, $T = \varphi(\rho, t)$, then the field is called one-dimensional, in the case under consideration, that is, when the liquid metal is cooled in a circular cylindrical crystallizer, it is convenient to take a cylindrical coordinate system ρ , θ , z , and consider the temperature field one-dimensional, since heat removal will mainly occur in the radial directions ρ , i.e. from the axis of symmetry to the walls of the mold (Figure 1).

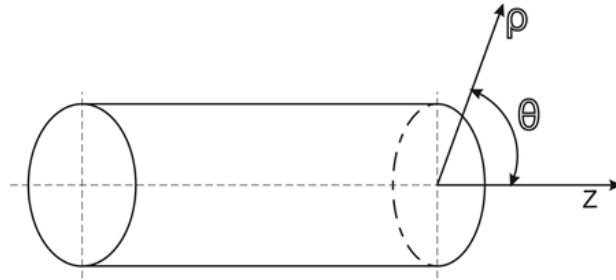


Fig. 1. - Adopted cylindrical coordinate system ρ , θ , z for describing the temperature field

The locus of points having the same temperature forms an isothermal surface. In Figure 1, individual points in the space of liquid metal in the mold, which have the same temperature, are interconnected by a line - isotherm.

Considering two isotherms with temperatures T and $T + \Delta T$ (Fig. 2), we can draw the following conclusion that at a specific point (for example, at point O), the sharpest temperature change is observed in the direction of the normal n to isothermal surfaces (Fig. 2).

As is known, thermal conductivity - is the process of heat propagation through direct contact of particles in the body. Thermal conduction transfers heat in gases, liquids and solids.

The basic law of heat propagation by heat conduction has the form:

$$g = -\lambda \text{grad} T, \quad (1)$$

where g - surface heat flux density, W/m^2 ; λ - thermal conductivity, $W/(m \cdot K)$.

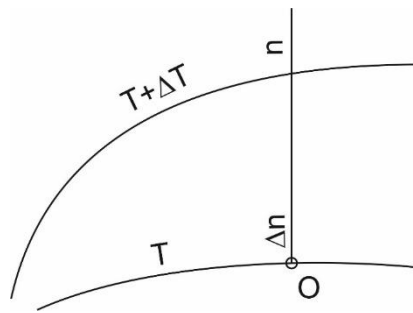


Fig. 2. - Determination of the temperature gradient

Thermal conductivity λ is a physical parameter of a substance that depends on the properties of a body, such as, for example, structure, bulk density, pressure, temperature. For metals, the value of thermal conductivity varies in the following limits $\lambda = 2 \dots 360 \text{ W}/(m \cdot K)$, and with an increase in temperature λ for most metals decreases.

With a non-stationary temperature field, a change in body temperature occurs, i.e. the body heats up or cools down. The rate of change in body temperature is characterized by the coefficient of thermal diffusivity, m^2/s :

$$a = \lambda / (c \cdot \gamma), \quad (2)$$

where c – specific heat of the body;

γ – body density.

The higher the values of a , the faster the temperature changes.

The change in body temperature in a nonstationary three-dimensional temperature field is expressed by the following differential equation:

$$\frac{dT}{dt} = a \left(\frac{d^2 T}{d\rho^2} + \frac{d^2 T}{d\theta^2} + \frac{d^2 T}{dz^2} \right). \quad (3)$$

To solve this differential equation, it is necessary to set the boundary conditions, which in this case are the sum of the time and boundary conditions.

Let us return to the considered process of metal cooling in a cylindrical mold, where heat is removed in the radial direction ρ , and the above differential equation (3) can be represented as follows:

$$\frac{dT}{dt} = a \frac{d^2T}{d\rho^2}. \quad (4)$$

In turn, the flow in an isotropic medium in an arbitrary direction n is associated with a change in temperature T by the following relation:

$$G_n = -a (\partial T / \partial n). \quad (5)$$

Now the next problem is to solve this differential equation (4) in relation to the given problem. For this, it is necessary to apply mathematical methods, in particular, numerical methods. Among the numerical methods for solving problems of mathematical physics, difference methods are widely used, among which, to solve this differential equation (4), we can apply the method of finite differences or the method of grids (MFD). When using these methods, the region under consideration is approximated by the grid region, and the values of the derivatives of the sought functions are replaced by difference relations through the values of these functions at the grid nodes. Further, for each node of the grid domain, the corresponding difference analogs of the original functional equations are compiled, the difference analogs of the given boundary conditions are compiled, and the problem is reduced to solving the system of algebraic equations.

To construct the simplest difference approximations of functions in the one-dimensional case, we write the expression for the function $f(\rho)$ in a small neighborhood $\rho + \Delta\rho$ using its expansion in the Taylor series:

$$f(x + \Delta x) = f(x) + f'(x)\Delta x + f''(x)\frac{\Delta x^2}{2!} + f'''(x)\frac{\Delta x^3}{3!} + \dots \quad (6)$$

Let the function $f_i(x)$ be given in the form of a table $f_i = f(x_i)$ ($i = 0, 1, \dots, n$), $\Delta x = x_{i+1} - x_i$. Then, limiting ourselves to two terms of the expansion, we can write

$$f_{i+1} = f(x_i + \Delta x) = f_i + f'_i \Delta x + \frac{f'' \Delta x^2}{2} \Big|_{i+\theta},$$

где $\theta = 0 \leq \theta \leq 1$

$$f'_i = \frac{f_{(i+1)} - f_i}{\Delta x} - f'' \frac{\Delta x}{2} \Big|_{i+\theta}$$

or

$$f'_i = \frac{f_{i+1} - f_i}{\Delta x} + O(\Delta x) \quad (7)$$

The error of this formula is of the order:

$$|E| \leq \frac{\Delta x}{2} \max |f''|_{i,i+1}.$$

Such a representation of the derivative is called the approximation of the first derivative by the difference forward. A similar expression can be obtained for the approximation by the derivative by the difference back:

$$f'_i = \frac{f_i - f_{i-1}}{\Delta x} + O(\Delta x) \quad (8)$$

To obtain more accurate formulas, you can represent the expression for the functions at the nodes $i-1$ and $i+1$ in the form:

$$f_{i+1} = f_i + f'_i \Delta x + f''_i \frac{\Delta x^2}{2} + f'''_i \frac{\Delta x^3}{6} \Big|_{i+\theta_1}, \quad 0 \leq \theta_1 \leq 1 \quad (9)$$

$$f_{i-1} = f_i - f'_i \Delta x + f''_i \frac{\Delta x^2}{2} - f'''_i \frac{\Delta x^3}{6} \Big|_{i-\theta_2}, \quad 0 \leq \theta_2 \leq 1 \quad (10)$$

Subtracting these equalities from one another, you can get:

$$f'_i = \frac{f_{i+1} - f_{i-1}}{2\Delta x} + O(\Delta x^2) \quad (11)$$

The error E of this approximation is determined $|E| \leq \frac{\Delta x^2}{6} \max|f'''|_{i-1, i+1}$.

Keeping in expressions (9), (10) the terms containing f''' and adding the results, we can obtain the difference expression for the second derivative

$$f''_i = \frac{f_{i+1} - 2f_i + f_{i-1}}{\Delta x^2} + O(\Delta x^2) \quad (12)$$

where $|E| \leq \frac{\Delta x^2}{12} \max|f''''|_{i-1, i+1}$.

In a similar way, one can construct difference expressions for higher-order derivatives:

$$f'''_i \cong \frac{f_{i+2} - 2f_{i+1} + 2f_{i-1} - f_{i-2}}{2\Delta x^3} \quad (13)$$

$$f''''_i \cong \frac{f_{i+2} - 4f_{i+1} + 6f_i - 4f_{i-1} + f_{i-2}}{\Delta x^4} \quad (14)$$

A similar technique can be used to construct difference approximations of partial derivatives in two-dimensional and spatial cases. In particular, on a two-dimensional grid in the vicinity of a node with indices i, k the second-order partial derivatives of the function $f(\rho, y)$ can be written in the form:

$$\frac{\partial^2 f}{\partial x^2} \cong \frac{f_{i+1, k} - 2f_{i, k} + f_{i-1, k}}{\Delta x^2} \quad (15)$$

$$\frac{\partial^2 f}{\partial y^2} \cong \frac{f_{i, k+1} - 2f_{i, k} + f_{i, k-1}}{\Delta y^2} \quad (16)$$

$$\frac{\partial^2 f}{\partial x \partial y} \cong \frac{f_{i+1, k+1} + f_{i-1, k-1} - f_{i-1, k+1} - f_{i+1, k-1}}{4\Delta x \Delta y} \quad (17)$$

To determine and construct the temperature field and the cooling time of the liquid metal in the mold, it is necessary to determine the function $T(\rho, t)$, which satisfies the above differential equation (9).

For all internal points of the mesh of the solidifying workpiece, a finite-difference analogue of the original differential equation (9) is compiled based on the use of the formulas of the method of finite difference (MFD):

$$\frac{T_{i+1} - 2T_i + T_{i-1}}{T_{i+1} - T_i} = \frac{\Delta \rho^2}{a_i(t_i - t_{i-1})}. \quad (18)$$

To solve MFD problems, the segment on which there is a function is divided by a certain number of equidistant grid points with coordinates, as shown in the Figure 3:

$\rho_i (i=0 \dots L)$, wherein $\rho_0=0, \rho_L=L, \rho_{i+1} - \rho_i = \Delta \rho, t_i (K=0 \dots K), t_0=0, t_K=K, t_{i+1} - t_i = \Delta t$.

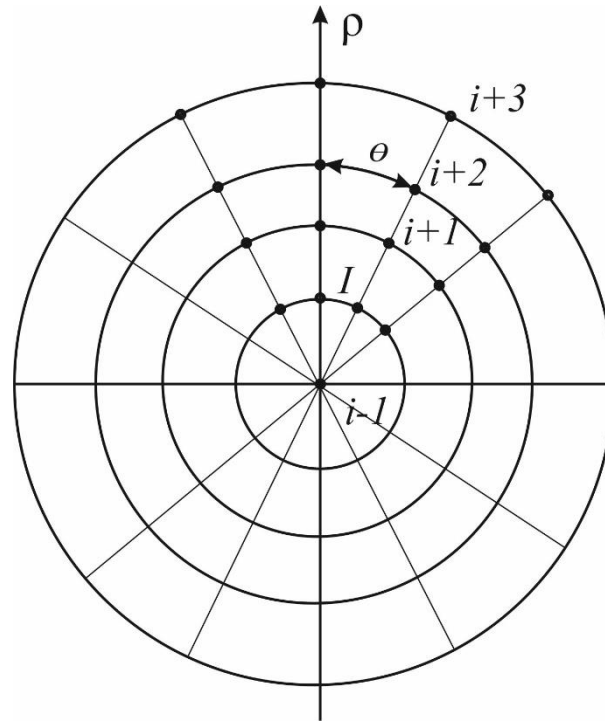


Fig. 3. - Nodes of the mesh applied to the cross-section of the mold blank

If the temperature values T^*0 and T^*L are known at both ends of the segment, then in the first and last nodes the equations are not compiled, and in the second and subsequent equations the known temperature values are transferred to the right side. Hence, the differential equation can be represented in the finite-difference form in the following form:

$$\left. \begin{aligned} \frac{T_2 - 2T_1 + T_0^*}{T_2 - T_1} &= \frac{\Delta\rho^2}{a_1\Delta t}; \\ \frac{T_3 - 2T_2 + T_1}{T_3 - T_2} &= \frac{\Delta\rho^2}{a_2\Delta t}; \\ \frac{T_4 - 2T_3 + T_2}{T_4 - T_3} &= \frac{\Delta\rho^2}{a_3\Delta t}; \\ \frac{T_5 - 2T_4 + T_3}{T_5 - T_4} &= \frac{\Delta\rho^2}{a_4\Delta t}. \end{aligned} \right\}$$

The result is $L-1 = 4$ algebraic equations for $L-1$ unknown values of t_i at the nodes of the stack area.

Solving the obtained algebraic equation for the cooling time Δt_i and t_i , we obtain the following.

We accept the change or step of the coordinate $\Delta\rho = 5$ mm or 0.005 m in a mold with an inner diameter of 40 mm, i.e. with respect to the axis of symmetry of the mold, the inner radius is divided from 0 by a step of 5 mm as follows: $\rho_0 = 0$, $\rho_1 = 5$ mm, $\rho_2 = 10$ mm, $\rho_3 = 15$ mm and $\rho_4 = 20$ mm. It is necessary to know the value of the temperature on the wall of the mold at $\rho_4 = 20$ mm. For calculations, we also take aluminum as the processed material, the physical properties of which are as follows: specific heat at $T=20^\circ\text{C}$, $c = 929, 46$ J/(kg*K), at $T=200^\circ\text{C}$, $c = 931,98$ J/(kg*K); thermal conductivity at $T=20^\circ\text{C}$ $\lambda = 217,0$ W/(m*K), at $T=200^\circ\text{C}$ $\lambda = 343$ W/(m*K), material density $\gamma=2700$ kg/m³, melting temperature $T_m = T_0 = 660^\circ\text{C}$.

In the study of these phenomena, an important role is played by research methods of the process of casting and extrusion of workpieces. To determine and construct temperature fields, the basic equations of heat conduction were used, and to solve these equations of heat conduction, numerical methods of the mathematical apparatus were used. In addition to the mathematical apparatus, a computer and graphic construction of the mechanism for filling the matrix cavity with solidifying metal was used.

To test the effectiveness of a new method of combining casting and extrusion in laboratory conditions, methods of physical modeling of a new process and a laboratory device for its implementation were used. As a modeling material,

we chose plasticine, plasto-paraffinic and other materials that simulate metals well under the appropriate temperature and velocity conditions.

It should be noted that some material processing processes cannot be implemented and studied in production conditions, especially fundamentally new technological processes and machine devices.

Therefore, it is advisable to study this or that issue in advance on models or modeling samples in a wide range of changes in various technological parameters and factors. Further, the results obtained in laboratory conditions are recalculated from model to nature. Then, in production conditions, at minimal cost, verification experiments are carried out in a limited number.

Such experimental studies are carried out to determine the main speed, kinematic parameters of the installation for combining casting and extrusion, to study the shape change of the resulting products.

It should be noted that it is convenient to carry out experiments on installations of lower power and on samples of smaller dimensions in comparison with full-scale dimensions.

3. Conclusions

Therefore, in order to extend the obtained experimental quantitative data to production conditions, it is necessary to observe the similarity of both processes.

Among all the conditions of similarity, it is easy to implement geometric similarities, where the ratios of the linear dimensions are taken to be the same and are convenient for implementation in low power conditions. In this case, the corresponding matrices and punches should also be geometrically similar, the ratio of their linear dimensions should be equal and correspond to linear samples of model samples.

It is much more difficult to maintain physical similarity, where it is necessary that the physical properties of the model and the nature should be the same in the initial state and at every moment of processing.

In addition, an important condition is compliance with speed parameters, i.e. speeds of movement of the main interconnected units of the machine for combining casting and extrusion. In this case, the duration of extrusion of the nature and the model should be the same: $\tau_M = \tau_H$.

To simulate or describe the method of combining casting and extrusion, a graphical method was used [4, 5].

4. References

- [1] Proceedings of the International Scientific and Practical Conference "Integration of Science, Education and Industry - the Basis for the Implementation of the Plan of the Nation" (Saginov's readings No. 9), 22-23 June 2017. In 4 parts. Part 3 / Ministry of Education and Science of the Republic of Kazakhstan, Karaganda State Technical University. - Karaganda: Publishing house of KSTU, 2017. – P. 347 - 349.
- [2] Proceedings of the International Scientific and Practical Conference "Integration of Science, Education and Industry - the Basis for the Implementation of the Plan of the Nation" (Saginov's readings No. 9), 14-15 June 2018. In 5 parts. Part 5 / Ministry of Education and Science of the Republic of Kazakhstan, Karaganda State Technical University. - Karaganda: Publishing house of KSTU, 2018. – P. 54 - 56.
- [3] Proceedings of the International Scientific and Practical Conference "Integration of Science, Education and Industry - the Basis for the Implementation of the Plan of the Nation" (Saginov's readings No. 11), 14-15 June 2019. In 5 parts. Part 5 / Ministry of Education and Science of the Republic of Kazakhstan, Karaganda State Technical University. - Karaganda: Publishing house of KSTU, 2019. – P. 201 - 204.
- [4] Zh.A. Ashkeyev, S.A. Mashekov, Zh.U. Bukanov. Filling the die cavity with solidifying metal when casting and extrusion processes are combined. Foundry, №2, 2020. – P. 34 - 36.
- [5] Zh.A. Ashkeyev, Zh.U. Bukanov. Calculation of the cooling time of cast billets in a cylindrical mold. Metallurgy of mechanical engineering, №5, 2017. – P. 32 - 34.

Information of the authors

Bukanov Zhanat Umirtaevich, senior lecturer at the department of nanotechnology and metallurgy of Karaganda technical university

E-mail: heissen69@mail.ru

Research of the Mechanism of Hardening of Liquid Metal in a Crystallizer During Casting and Extrusion Machine

Ashkeyev Zh.A.*

Karaganda Industrial University, Temirtau, Kazakhstan

*corresponding author

Abstract. The article examines the mechanism of solidification of liquid metal in a mold when working on a casting and extrusion machine. The synchronicity of movement of the machine slider is investigated. A diagram of the formation of a cast billet upon cooling in a mold and extrusion of the solidifying metal into the cavity of the matrix is given. Diagram of extrusion of a solidified crust with a thickness of δ through the formed gap. Graph of changes in the dependence of the formation of a "healthy" crust on time.

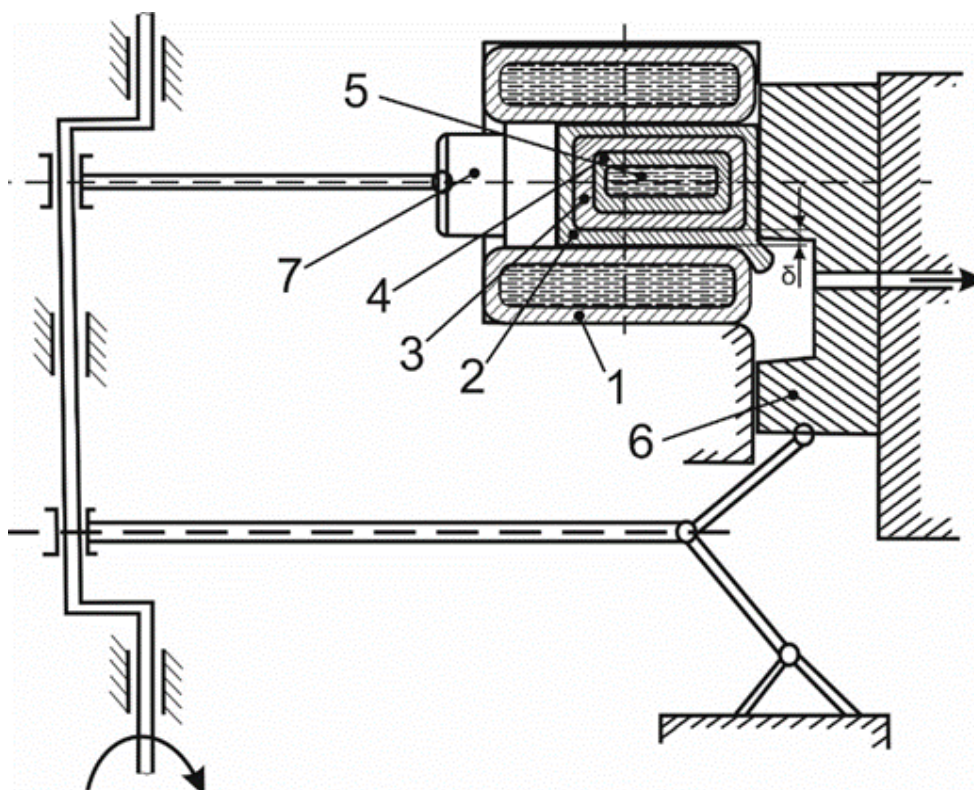
Keywords: crystallizer, casting, heading, cooling, liquid metal.

1. Introduction

Of great importance at the current stage of development of the metallurgical and machine-building industry is the creation of casting and heading machines (CHM) of a new generation, as the most progressive and promising in the production of various parts and blanks.

We investigate the processes occurring during the operation of the casting and extrusion machine. Earlier, the developed design of the machine itself was reported at international practical conferences [1-3], and published in journals of neighboring countries [4, 5].

The technological cycle is shortened due to the fact that instead of metal rolling, cast billets obtained by solidifying the metal in a water-cooled mold and with its subsequent extrusion into the cavity of the matrix are used as initial blanks. The synchronous movement of the slider 7 of the machine, which delivers the solidifying workpiece to the slightly opening cavity of the matrix to fill it with the solidifying metal, is carried out due to the work of the interconnected links of the machine (Figure 1).



1 – crystallizer, 2,3,4 – gradually forming crust, 5 – liquid phase, 6 – matrix, 7 – slider

Fig. 1. - Scheme of the formation of a cast blank during cooling in a mold and extrusion of solidifying metal into the cavity of the matrix

Hence the problem of ensuring synchronous movement of the slider 7 and the matrix 6 with the time of cooling the metal in the mold and opening the cavity of the matrix, i.e. the process of filling the matrix cavity with solidifying metal. Therefore, we tried to explain the method of filling the matrix cavity with a gradually solidifying metal.

2. Results and discussion

It is known that the crystallization of liquid metal (LM) begins from the wall of the water-cooled crystallizer 1 and is formed in the direction of heat removal, starting from the wall of the crystallizer in the radial direction, as a result of which a "healthy" crust 2 crystallizes and forms, then 3 and 4. At the initial stage, a liquid phase 5 will still remain in the core. But in this case, the volume of the liquid phase will gradually decrease, which is undesirable, since all impurities will shift towards the LM.

Hence, based on the proposed method of crystallization of LM in the crystallizer, it can be assumed that the first solidified crust 2 formed in the form of a tube will be squeezed out first, the next will be squeezed out into the gradually opening cavity of the matrix the next solidified crust 3, 4, etc. In this case, it is possible that liquid phase 5 will also be retained (Fig.1).

In this case, the synchronization of the formation of the hardened crust and the gradual opening of the matrix cavity due to its movement upward, as the machine slider moves, is important, which implies the coincidence of the time t of the formation of a healthy hardened crust (layer) of metal with a thickness of δ and the opening of the gap of the matrix cavity during this time interval t and extrusion of the hardened layer into this cavity. This is a very important point that must be considered.

It turns out that the solidification of a metal layer ~ 1 mm thick requires $1 \dots 1,5$ s. It is with this interval that it is necessary to associate the time of movement of the slider and the matrix by choosing the time of rotation of the cranks. It should be noted that during the time t of the formation of the solidified layer, the cavity of the matrix should open slightly by the size of the solidified metal layer δ . Suppose, if a circular cylindrical workpiece is extruded, then the slightly opened gap (or slot) will have the shape of an oval, the semi-minor axis of which will be equal to 0.5δ . (fig. 2). It should be assumed that a high extrusion pressure will be observed in the initial period of extrusion, and as the gap further increases due to the opening of the die cavity, the pressure will gradually decrease, since the area of the oval will increase more and more, i.e. the gap of the oval will initially be equal to δ_1 , then $\delta_2 \dots \delta_N$, where N – the ordinal number of the solidified layer.

Calculations have shown that compressive stresses (pressures) of 88.9 MPa or ~ 9 kgf / mm² act at the exit of the solidified metal from the mold into the die cavity, which can be realized with the correct choice of the machine drive to combine the casting and extrusion processes. For example, if a crust of a metal layer 5 mm thick has formed, then the force of extrusion of the metal layer formed at the initial stage into the slightly opened oval gap will be:

$$P = S\sigma_{bx} = \pi 0,5 \cdot 5^2 \cdot 54,35 = 2133,2\text{H or } \sim 213 \text{ kgf.}$$

The resulting force of extrusion of the formed metal layer may well be realized by the drive of the machine at the initial stage of crystallization of the cast blank.

Now it is necessary to determine the time of solidification of the formed crust of thickness δ in the mold. To do this, we use the basic equations of physics and heat conduction.

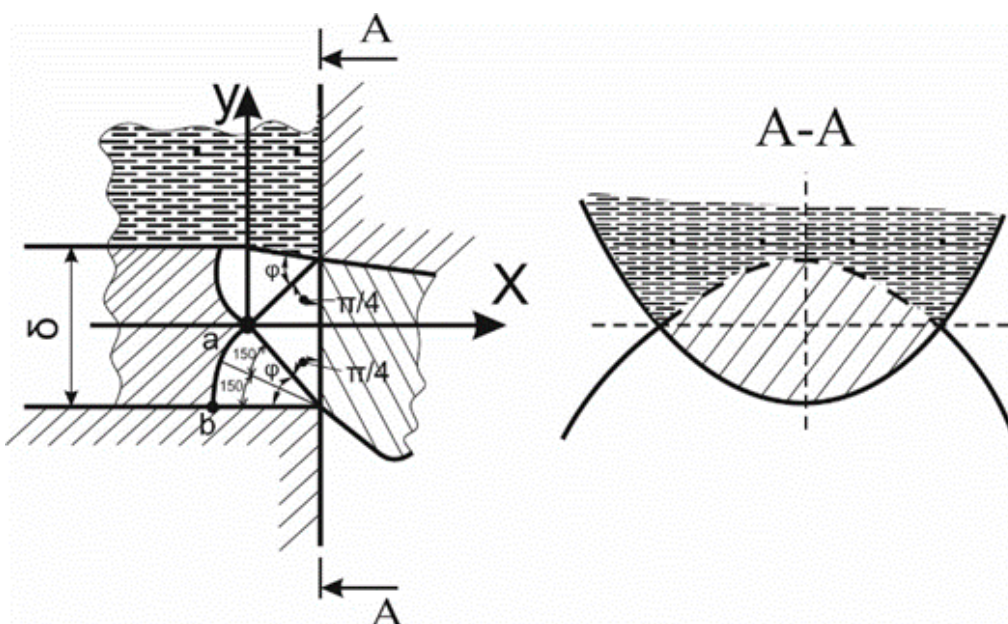


Fig. 2. - Diagram of squeezing out the hardened crust thickness δ through the formed gap

Thus, the time of formation of a "healthy crust" (Fig. 3):

- first crust $\delta_1, t_1 = 5,25s$,
- second crust $\delta_2, t_2 = 13,12s$,
- third crust $\delta_3, t_3 = 17,52s$,
- fourth crust $\delta_4, t_4 = 20,05s$.

Full solidification time of the cast blank:

$$t_{gen.} = \Delta t_1 + \Delta t_2 + \Delta t_3 + \Delta t_4 = 5,25 + 7,87 + 4,48 + 2,53 = 20,13s.$$

Analysis of the results obtained shows that the extrusion process for aluminum can be started in 5 seconds, i.e. after the formation of the first crust $S_1 \approx 5mm$, it is necessary to relate to the time of movement of the slider and the matrix of the machine in order to completely complete the process. To do this, you need to know the stroke and stroke time: S, V, t the dependence of which can be expressed: $dV = \frac{dS}{dt}$, from here you can determine the time and agree with the solidification time of the liquid metal, which is described in more detail in the articles [1-5].

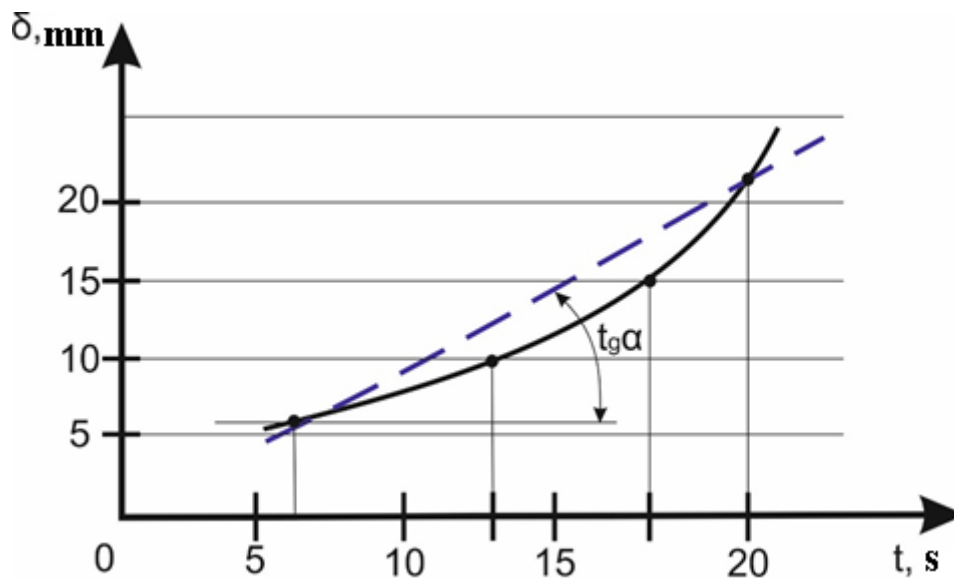


Fig.3. - Graph of changes in the dependence of the formation of a "healthy" crust from time to time

On the basis of the results obtained, a general view of a machine for combining casting and extrusion or a casting-extruding machine (CEM) is proposed (Fig. 4). In addition to the main, executive parts in Fig. 4 shows other auxiliary parts of the machine: a bracket, connecting pins, a gas outlet, which also serves to push the solidified metal out of the die cavity.

The machine consists of a closed box 1 of a rectangular shape, which is a support for all parts of the machine, i.e. the following main units of the machine are attached to the body: crank – 2, which performs a reciprocating motion; the connecting rod - 3 and the connecting rod - 8, with the help of which the operation of extruding the blanks is performed and on which the yokes - 4 and the slider - 9 are connected; water-cooled crystallizer - 7, where liquid metal is poured; matrix holder - 5 and matrix - 6. To connect the connecting rod - 3 and yokes - 4, a connecting hook - 3 and a pin - 10 are provided, the other end of the yokes is connected to the matrix holder - 5 and the bracket on the machine body - 11.

The dimensions of the main parts of the matrix, in particular the crank, connecting rod, yokes, were preliminarily taken, which should be checked for strength using a technique known from the theory of strength and elasticity.

In order to show the performance of the proposed machine designs, we first perform modeling and animation in two ways: graphic and computer.

The principle of operation of the machine for casting and extrusion is as follows: 1) when the drive rotates, the crank 2 starts to move simultaneously the connecting rods 3 and 8, which move the slider 9 and the matrix holder 5 together with the matrix 6 due to the interconnected levers 4, starting from the left extreme point to the right the extreme point towards each other, 2) at the moment of filling the cavity of the matrix with the solidifying metal, the slider and the matrix holder together with the matrix, reaching the right extreme right position, from this point begin to move in the opposite direction, 3) when the slide and the matrix move in the opposite direction, the pressed workpiece is pushed out of the die cavity through the gas outlet. Then the process is repeated again.

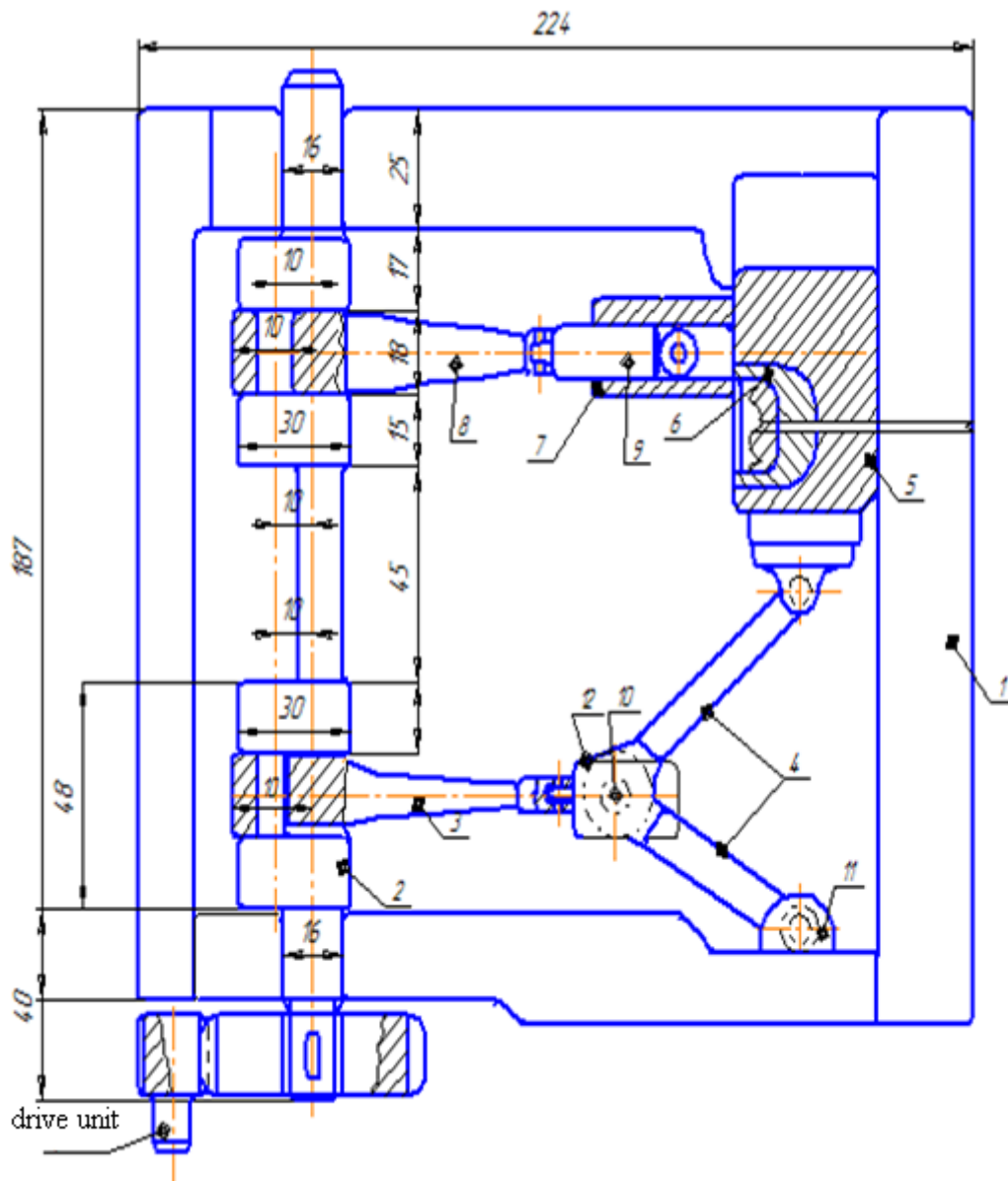


Fig. 4. - General view of the machine for injection and extrusion

To simulate or describe the method of combining casting and extrusion, a graphical method was used in the CorelDraw.

3. Conclusions

- 1) An equation for the total solidification time of the cast billet is obtained;
- 2) The dependences of the formation of a "healthy" crust on time were obtained for liquid metal (aluminum);
- 3) A drawing of the machine for combining casting and extrusion has been developed.

4. References

- [1] Proceedings of the International Scientific and Practical Conference "Integration of Science, Education and Industry - the Basis for the Implementation of the Plan of the Nation" (Saginov's readings No.9), 22-23 June 2017. In 4 parts. Part 3 / Ministry of Education and Science of the Republic of Kazakhstan, Karaganda State Technical University. - Karaganda: Publishing house of KSTU, 2017. - P. 347 - 349.
- [2] Proceedings of the International Scientific and Practical Conference "Integration of Science, Education and Industry - the Basis for the Implementation of the Plan of the Nation" (Saginov's readings No.9), 14-15 June 2018. In 5 parts. Part 5 / Ministry of Education and Science of the Republic of Kazakhstan, Karaganda State Technical University. - Karaganda: Publishing house of KSTU, 2018. - P. 54 - 56.
- [3] Proceedings of the International Scientific and Practical Conference "Integration of Science, Education and Industry - the Basis for the Implementation of the Plan of the Nation" (Saginov's readings No.11), 14-15 June 2019. In 5 parts. Part 5 / Ministry of Education and Science of the Republic of Kazakhstan, Karaganda State Technical University. - Karaganda: Publishing house of KSTU, 2019. - P. 201-204.

- [4] Ashkeyev Zh.A., Mashekov S.A., Bukanov Zh.U. Filling the die cavity with solidifying metal when casting and extrusion processes are combined. Foundry. No.2, 2020. – P. 34-36.
- [5] Ashkeyev Zh.A., Bukanov Zh.U. Calculation of the cooling time of cast billets in a cylindrical mold. Metallurgy of mechanical engineering. No.5, 2017. – P. 32-34

Information of the authors

Ashkeev Zhasulan Amanzholovich, candidate of technical sciences, associate professor of the department “Metal forming” of Karaganda Industrial University
E-mail: jashkeev@mail.ru